BEHAVIOR OF LINED OPENINGS IN JOINTED AND UNJOINTED MODEL ROCK MASSES

James G. Wallace

Army Engineer Waterways Experiment Station
Vicksburg, Mississippi

September 1973

TECHNICAL REPORT N-73-6

BEHAVIOR OF LINED OPENINGS IN JOINTED AND UNJOINTED MODEL ROCK MASSES

by

J. G. Wallace

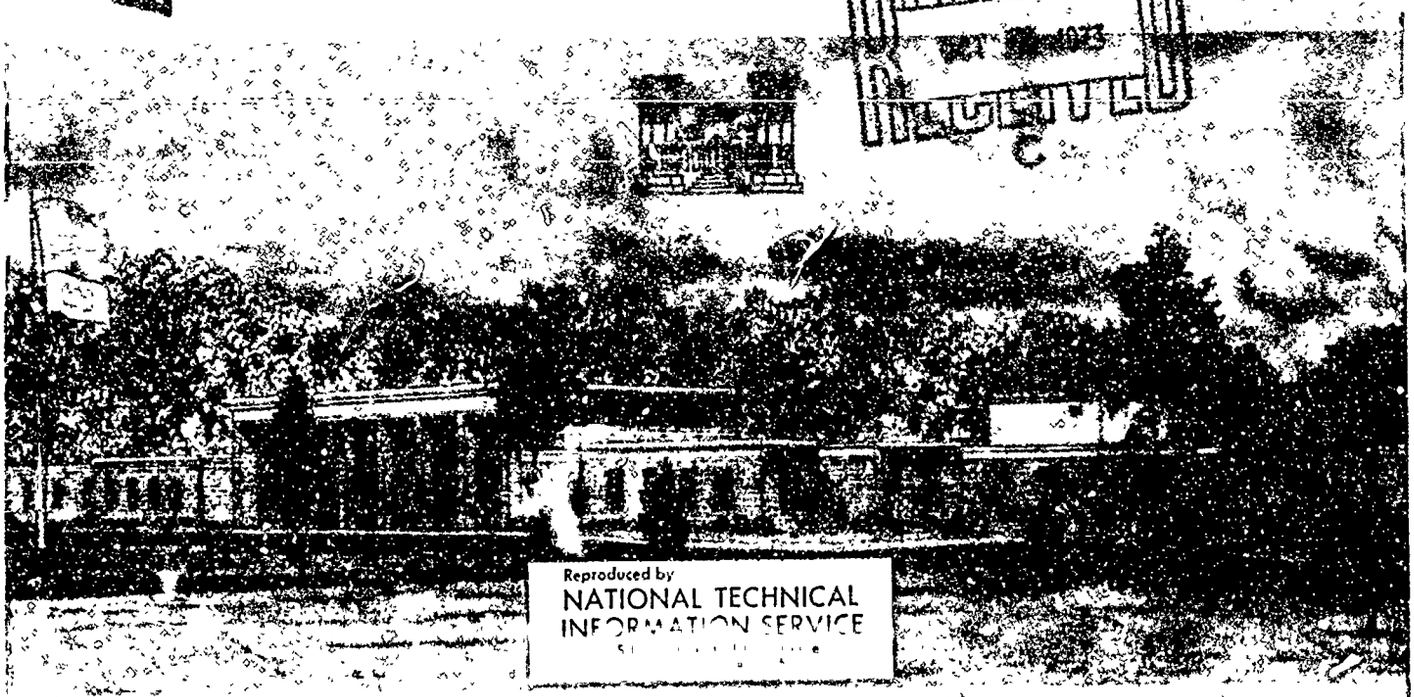

September 1973

Sponsored by Office, Chief of Engineers, U. S. Army

Conducted by U. S. Army Engineer Waterways Experiment Station
Weapons Effects Laboratory
Vicksburg, Mississippi

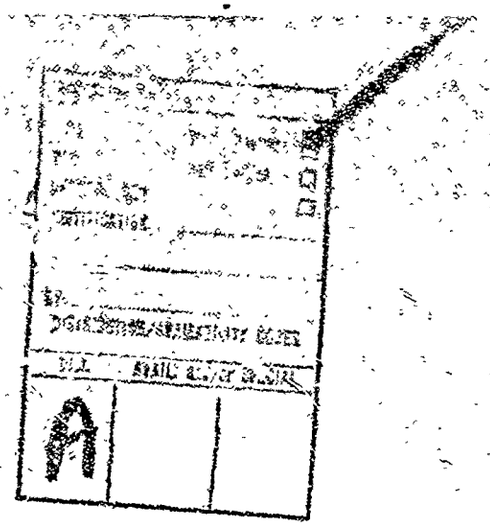

Destroy this report when no longer needed. Do not return it to the originator.

The findings in this report are not to be construed as an official Department of the Army position unless so designated by other authorized documents.

Unclassified
Security Classification

DOCUMENT CONTROL DATA - R & D

(Security classification of title, body of abstract and indexing annotation must be entered when the overall report is classified)

1 ORIGINATING ACTIVITY (Corporate author) U. S. Army Engineer Waterways Experiment Station Vicksburg, Mississippi	2a. REPORT SECURITY CLASSIFICATION Unclassified 2b. GROUP

3 REPORT TITLE

BEHAVIOR OF LINED OPENINGS IN JOINTED AND UNJOINTED MODEL ROCK MASSES

4 DESCRIPTIVE NOTES (Type of report and inclusive dates)

Final report

5 AUTHOR(S) (First name, middle initial, last name)

James G. Wallace

6. REPORT DATE	7a. TOTAL NO. OF PAGES	7b. NO. OF REFS
September 1973	~~57~~ 59	13

8a. CONTRACT OR GRANT NO b. PROJECT NO A880 c. d.	9a. ORIGINATOR'S REPORT NUMBER(S) Technical Report N-73-6 9b. OTHER REPORT NO(S) (Any other numbers that may be assigned this report)

10 DISTRIBUTION STATEMENT

Approved for public release; distribution unlimited

Details of illustrations in this document may be better studied on microfiche.

11 SUPPLEMENTARY NOTES	12. SPONSORING MILITARY ACTIVITY Office, Chief of Engineers, U. S. Army Washington, D. C.

13 ABSTRACT

The objective of this investigation was to study experimentally the behavior of horizontally oriented, steel-lined cylindrical openings in jointed and unjointed model rock masses subjected to static surface overpressures. The results of six model tests are presented and discussed herein. Three of these tests were conducted on virgin jointed model rock masses containing steel-lined cylindrical openings. The other three tests were repeated loadings of an unjointed model rock mass containing a steel-lined opening. The boundary conditions were approximately plane stress conditions in all cases. The development of jointed model rock masses and the required instrumentation are also described herein. The behavior of the steel liners was measured with circumferential strain gages and diametric extensometers. The free-field response was measured with SE-type stress gages. Test results indicated that even widely spaced joints drastically influence the moments and diametrical movements of the tunnel liner, but that the thrust is not so grossly affected.

DD FORM 1 NOV 68 1473 REPLACES DD FORM 1473, 1 JAN 64, WHICH IS OBSOLETE FOR ARMY USE.

Unclassified
Security Classification

14 KEY WORDS	LINK A		LINK B		LINK C	
	ROLE	WT	ROLE	WT	ROLE	WT
Joints and jointing (geology)						
Lined tunnels						
Models						
Rock masses						
Static pressure						

THE CONTENTS OF THIS REPORT ARE NOT TO BE USED FOR ADVERTISING, PUBLICATION, OR PROMOTIONAL PURPOSES. CITATION OF TRADE NAMES DOES NOT CONSTITUTE AN OFFICIAL ENDORSEMENT OR APPROVAL OF THE USE OF SUCH COMMERCIAL PRODUCTS.

ABSTRACT

The objective of this investigation was to study experimentally the behavior of horizontally oriented, steel-lined cylindrical openings in jointed and unjointed model rock masses subjected to static surface overpressures.

The results of six model tests are presented and discussed herein. Three of the tests were conducted on virgin jointed model rock masses containing steel-lined cylindrical openings. The other three tests were repeated loadings of an unjointed model rock mass containing a steel-lined opening. The boundary conditions were approximately plane stress conditions in all cases.

The development of jointed model rock masses and the required instrumentation are also described herein. The behavior of the steel liners was measured with circumferential strain gages and diametric extensometers. The free-field response was measured with SE-type stress gages.

Test results indicated that even widely spaced joints drastically influence the moments and diametrical movements of the tunnel liner, but that the thrust is not so grossly affected.

PREFACE

The study reported herein was conducted in the 6,000-psi-capacity Static Test Device at the U. S. Army Engineer Waterways Experiment Station (WES) under the sponsorship of the Department of the Army, Office, Chief of Engineers (OCE), Military Construction Directorate, Nuclear Construction and Engineering Project A880 (NCE) Work Unit, "Vulnerability of Structures in Rock to Ground Motions from Nuclear Explosions." Mr. D. S. Reynolds was the OCE coordinator for this work unit.

This work was accomplished during the period June 1969 through April 1973 under the general supervision of Mr. G. L. Arbuthnot, Jr., and Mr. W. J. Flathau, Chiefs of the Weapons Effects Laboratory, WES, and under the direct supervision of Mr. L. F. Ingram, Chief, Phenomenology and Effects (P&E) Division. This report was prepared by Mr. J. G. Wallace of the P&E Division. The suggestions and assistance of Messrs. C. E. Joachim, J. L. Drake, C. M. Wright, and J. A. Conway are appreciated.

COL L. A. Brown, CE, BG E. D. Peixotto, CE, and COL G. H. Hilt, CE, were Directors of the WES during the conduct of this study and preparation of this report. Mr. J. B. Tiffany and Mr. F. R. Brown were Technical Directors.

CONTENTS

TABLES

FIGURES

NOTATION

a	Outside radius of the steel cylinders, inches
b	Horizontal joint spacing, inches
d	Vertical joint spacing, inches
E	Young's modulus of elasticity, psi
EI/R^3	Average cylinder stiffness, psi
I	Moment of inertia per unit length of steel cylinder, in^4/in
M	Circumferential bending moment per unit length of cylinder, in-lb/in
P	Applied surface pressure, psi
q_u	Unconfined compressive strength
r	(Subscript) model rock
R	Radial distance from the centerline of the cylinder, inches
t	Steel cylinder wall thickness, inches
T	Circumferential thrust per unit length of cylinder, lb/in
γ	Average density, pcf
ϵ_e	Exterior circumferential cylinder strain, percent
ϵ_i	Interior circumferential cylinder strain, percent
θ	Angle measured at the center of the cylinder cross section positive clockwise from the crown, degrees
ν	Poisson's ratio
σ	Circumferential stress, psi
σ_h	Free-field horizontal pressure, psi
σ_r	Radial stress, psi
σ_t	Tensile strength of model rock, psi
σ_v	Free-field vertical pressure, psi
ϕ	Angle of internal friction of model rock material, degrees

CONVERSION FACTORS, BRITISH TO METRIC UNITS OF MEASUREMENT

British units of measurement used in this report can be converted to metric units as follows:

Multiply	By	To Obtain
inches	2.54	centimeters
feet	0.3048	meters
cubic feet	0.0283168	cubic meters
pounds (mass)	0.45359237	kilograms
pounds (force) per square inch	0.6894757	newtons per square centimeter
pounds (mass) per cubic foot	16.0185	kilograms per cubic meter
inch-pounds	0.011521	meter-kilograms
inches per second	2.54	centimeters per second
Fahrenheit degrees	5/9	Celsius or Kelvin degrees[a]

[a] To obtain Celsius (C) temperature readings from Fahrenheit (F) readings, use the following formula: $C = 5/9 (F - 32)$. To obtain Kelvin (K) readings, use: $K = 5/9 (F - 32) + 273.15$.

CHAPTER 1

INTRODUCTION

1.1 BACKGROUND

In the past decade, a concerted effort has been made to develop design criteria for deep underground cavities subjected to nuclear-weapon-induced ground shock. In spite of this effort, additional basic studies are required before a rational design methodology can be formulated.

The curtailment of atmospheric nuclear testing and the cost of conducting full-scale underground tests have necessitated the development of laboratory techniques and facilities to study the response of buried protective structures subjected to nuclear threats. Practical limitations on the size of the laboratory facilities such as loading apparatus require that the testing be conducted on small-scale models of prototype structures. The theory of similitude is useful in planning the tests, interpreting the results, and formulating design criteria.

In this study, emphasis was placed on horizontally oriented cylindrical structures which form an integral part of many underground strategic systems such as command capsules, ventilation tunnels, and underground adits connecting central facilities in super-hard defensive complexes.

1.2 OBJECTIVES OF INVESTIGATION

The general objective of this investigation was to add to the present knowledge of the strength, behavior, and failure of lined cylindrical openings in a jointed rock medium.

Specifically, the objectives were (1) to develop a model rock material, (2) to study the effect of joint spacing on the thrust bending moment and diameter changes of a structural liner in a jointed medium, and (3) to study the free-field pressure distribution.

1.3 SCOPE OF STUDY

Most rock masses in which underground protective structures are built contain discontinuities. This investigation is a study of the interaction of cylindrical tunnel liners with a jointed model rock mass.

To accomplish the objectives of the study, a model rock material was developed and six tests were conducted on jointed and unjointed model rock masses containing steel-lined cylindrical openings.

The effects of joint spacing on medium-structure interaction was the primary parameter investigated. In order to study the full influence of jointing in the medium on tunnel behavior, it was considered that the ratio of tunnel diameter to joint spacing variation should be at least an order of magnitude. The ratios of tunnel diameter to joint spacing used in this study were two, four, and nine. An unjointed model rock mass was also included in the study. Measurements of circumferential strain; springline, crown-invert, and 45-degree diameter changes; overpressure; and free-field pressure were made.

1.4 REVIEW OF PREVIOUS STUDIES

Model studies of the behavior of underground openings in rock have been conducted by several investigators (References 1 through 8). These studies have resulted in various degrees of success in accurately and adequately simulating a prototype rock mass-structure interaction. Some of the studies were conducted to simulate prototypes, and others were conducted to study rock mass behavior in general. An extensive review of previous work in model rock studies is included in Reference 1. The primary shortcomings of most investigations have been inadequate model materials and test facilities.

CHAPTER 2

EXPERIMENTAL PROCEDURES

2.1 DESCRIPTION OF THE MODEL MATERIALS

2.1.1 General. The literature (References 9 through 12) indicates that the average properties of unjointed rock are generally such that:

$$0.05 \leq \frac{\sigma_t}{q_u} \leq 0.10 \; ; \quad 250 \frac{E}{q_u} \leq 500 \; ;$$

$$0.1 \leq \nu \leq 0.3 \; ; \quad 25 \text{ degrees} \leq \phi \leq 60$$

Where: σ_t = tensile strength
q_u = unconfined compressive strength
E = tangent modulus of elasticity
ν = Poisson's ratio
ϕ = angle of internal friction

These represent stringent requirements on the model rock material. In practice, these requirements are almost impossible to satisfy. The model rock material used in the tests described herein was adapted from a previously developed model material (Reference 6) that had undergone an extensive series of tests to determine its jointed and unjointed strength and deformation characteristics.

2.1.2 Model Rock Material Components. The model rock material used in this study was dense, fine, angular sand cemented with a gypsum matrix. A grain-size distribution curve for the sand is shown in Figure 2.1. The gypsum cement used was U. S. Gypsum Hydrocal B-11.

The standard mix used consisted of 76 percent sand, 10 percent Hydrocal B-11, and 14 percent water by weight.

2.1.3 Model Rock Material Preparation. The mixing and casting technique developed in the study described in Reference 6 was also used

in this study. A 500-pound[1]-capacity vibrating table with a 30- by 30-inch bed and a maximum amplitude of vibration of 0.025 inch was used to obtain the desired material density.

The small cylindrical specimens used to determine the engineering properties were cast in standard 3- by 6-inch steel molds clamped to the vibrating table with C-clamps.

The large intact blocks used to build up a jointed mass were cast in molds made of 0.500-inch-thick precision aluminum plate. The mold sizes were changed after each test to obtain the required joint spacing in the completed jointed model. Since gypsum chemically reacts with aluminum, it was necessary to spray the models with an inert epoxy paint to protect the mold surface. The mold release agent used to obtain smooth surfaces was a commercially available coating called Lift-a-Part.[2]

A 2-1/2-ft^3 concrete mixer was used to mix the material required for each batch. The same batch weight was cast each time with a vibration time of 5 minutes to insure uniformity of material density.

The specimens were cured under room conditions at 100 percent relative humidity and a temperature of 73 F for 3 days. Then the molds were removed and the specimens were placed in a controlled environment of 50 percent relative humidity and 115 F for a period of 14 days to remove the chemically free water. A drying curve for the 3- by 6-inch cylindrical specimens is shown in Figure 2.2.

2.1.4 Model Rock Material Properties. The same model rock material was used throughout this study. It was essentially a densely compacted, fine, angular sand cemented into a cohesive mass with a gypsum matrix. Mohr's failure envelope for the material is shown in Figure 2.3. Figure 2.3 shows that the model material had an average unconfined compressive strength q_u of 600 psi, a tensile strength σ_t of 10 percent of q_u, and an angle of internal friction ϕ of 29 degrees. Three specimens were used to obtain average stress-strain

---

[1] A table of factors for converting British units of measurement to metric units is presented on page 10.

[2] Imperial Chemical Company, 1460 West Hubbard, Chicago, Illinois.

curves at confining pressures of 0, 100, and 300 psi. These curves are presented in Appendix A. The measured values of Poisson's ratio ν_r varied from 0.15 to 0.35. The material had an average initial Young's modulus E_r of 1.0×10^6 psi and an average density γ of 121 pcf.

2.1.5 Description of Cylindrical Test Specimens. The cylindrical test specimens were fabricated from cold-drawn, low-carbon, seamless, mechanical steel tubing. The specimens had an outside diameter of 6 inches $\pm$1 percent and a wall thickness of 1/8 inch $\pm$2 percent. The average stiffness EI/R^3 of the cylinders was 170 psi. The steel had an elastic modulus of 30×10^6 psi, a proportional limit of 47,700 psi, and a rupture strength of 91,200 psi.

Figure 2.4 illustrates the test geometry of the cylinders. The central test section was 18 inches long. The closed-end caps were 8 inches long and were independently supported by three 3/4-inch-diameter, cold-drawn steel rods. The ends of the support rods were threaded, and nuts were used to maintain the separations between the central test section and the end caps. The separations between the end caps and the central test section were closed with a silicone rubber gasket.

The end conditions of the central test section were essentially stress-free boundaries, since the axial thrust was isolated from the central test section by the thrust isolation assembly shown in Figure 2.5.

2.1.6 Description of Test Configuration. Static tests were conducted on four 6-inch-O.D. steel cylinders with a wall thickness of 1/8 inch contained in jointed and unjointed model rock masses. The test section was 18 inches long and specially isolated from longitudinal thrust to approximately simulate a plane-stress condition, as shown in Figure 2.6.

The steel cylinders were tested in an unjointed model rock made up of 4-inch-thick slabs joined by a thin epoxy glue line in the horizontal plane. In addition, tests were conducted on jointed model rock masses having horizontal to vertical joint spacings, b/d, of 3/1, 3/2, and 2/3.

2.2 TESTING FACILITY

All testing was conducted in the WES 6,000-psi-capacity static testing device (Figure 2.7). The test chamber uses the Central Firing Station (CFS) of the LBLG as a reaction structure. The test chamber itself is a steel cylinder 46-3/4 inches in diameter and 42 inches high. It has a piston-type lid that seals the top and rests on a steel plate with an O-ring to seal the bottom. The testing device is composed of (1) a platen, (2) spacer blocks, (3) a test chamber, and (4) an upper bearing block. When the test chamber is inside the CFS, it is sandwiched between the upper bearing block and the spacer blocks.

An air-to-hydraulic multiplier is used to pressurize the test chamber. The pressure pushes the piston-type lid up until the upper bearing block makes full contact with the ceiling of the CFS. The upper bearing block and the platen distribute the load to the CFS. The test specimen is then loaded through a rubber diaphragm by water pressure supplied by an air-driven pump.

2.3 INSTRUMENTATION

2.3.1 Strain Measurements. Circumferential strain measurements were recorded at the midpoint of the steel cylindrical test section. They were measured with Micro-Measurement Type EA-06-250BG-120 SR-4 strain gages. These gages were 0.25 inch long with an electrical resistance of 120 ohms and were temperature-compensated for steel. The gages were placed on the interior and exterior surfaces of the central test sections at angles θ of 0, 30, 60, 90, 120, 150, 180, and 270 degrees (Figure 2.8). Temperature compensation was accomplished by internally completing a wheatstone bridge for each active sensing element with three dummy gages. The dummy gages were mounted on a stress-free, 1-1/4-inch-diameter steel bar which was cantilevered from one of the spacer plates (Figure 2.5).

The three thrust rods (Figure 2.5) supporting the closed-end caps were instrumented with four strain gages that were identical with those used on the central test section. Two of the gages were mounted longitudinally and diametrically opposite each other. The other two gages

were mounted circumferentially and diametrically opposite each other. The four gages were connected to form a wheatstone bridge which responded only to axial loads and provided automatic temperature compensation.

2.3.2 Deflection Measurements. Deflection gages similar to those used in the study described in Reference 13 were used to measure the relative displacements of the steel liner. The deflection transducers consisted of a 0.015-inch-thick, 1/4-inch-wide, 7-inch-long strip of beryllium copper bent into a "C" shape, with 1/4-inch-long tabs at each end. Two Micro-Measurement Type EA-06-250BG-120 strain gages were mounted on each side of the strip's center. The gages were electrically connected to indicate only bending strains. Small steel buttons were glued on the crown invert, springline, and 45-degree axis near the midpoint of the central test section. The instrumented shim-stock was bent and compressed like a spring and placed inside the liner, with the ends of the 1/4-inch-long tabs pushing out against the steel buttons glued to the liner wall (Figure 2.9).

Each deflection gage was calibrated in a compressed position for extension and compression on a Pratt and Whitney Super-Micrometer. The wheatstone bridge output was a linear function of the relative displacement of the ends, and, on a strain indicator, had a sensitivity of approximately 1 μin/in output per 0.0001 inch of diameter change.

2.3.3 Pressure Measurements. Free-field pressures were measured with WES SE thin diaphragm pressure transducers. A detailed evaluation of this type gage is presented in Reference 2. Horizontal and vertical pressure measurements were recorded across the midsections of the models parallel to the springline and crown invert axes. Pressure gage locations for all tests are presented in Figures 2.10 through 2.12. The static surface overpressure was measured with two 10,000-psi-capacity Dynesco pressure transducers.

2.3.4 Data Recording Equipment. Signal conditioning of the resistance-type wheatstone bridge circuits was accomplished with SAM amplifiers and B and F modules coupled with DANA amplifiers. Each system provided variable dc excitation voltage, automatic double-shunt

calibration, and amplifiers to meet the input requirements of the recording equipment.

Sangamo magnetic-tape recorders were used to record the analog output voltage signals from the tests. Each tape record had 14 data tracks and an edge voice track. A recording speed of 7-1/2 in/sec was used, and the playback speed was determined by the duration of the tests.

2.4 MODEL CONSTRUCTION

2.4.1 General. The completed model rock masses with steel-lined tunnels represented a complex assembly of components. The following sections describe the prodecures used during the assembly.

2.4.2 Test Cylinder Assembly. The central test section was placed over the thrust isolation assembly. Completion of the wheatstone bridges for the circumferential strain gages was accomplished internally by connecting them to the dummy gage block and terminal strips attached to the thrust rod assembly (Figure 2.5).

After the connections had been completed and the end caps attached, pliable gaskets were placed in the separation joints. The cylindrical test specimen was then strapped to a wooden cradle for handling purposes. A completed cylinder assembly is shown in Figure 2.13.

2.4.3 Construction of Jointed Model Rock Masses. The maximum external dimensions of the model rock masses used in this study were 34 by 34 by 34 inches. These dimensions were dictated by the size of the test facility.

The models were constructed from individual blocks of model material. All of the jointed models were constructed with two sets of mutually perpendicular joints oriented in the principal stress directions. The models were constructed on a 2-1/2-inch-thick steel plate which was used to handle the finished models. A partially completed model with the instrumented tunnel liner in place is shown in Figure 2.14. The joints adjacent to the liner were waterproofed with a thin coating of polyurethane paint. The liner was then grouted into place using a semi-liquid grout consisting of 60 percent fine sand, 15 percent hydrocal, and 25 percent water by weight to insure good initial contact between

the model and the tunnel liner. The SE pressure gages were installed as construction of the model assembly progressed. Due to the friable nature of the model rock material, this was a delicate operation. Holes were were carefully hand-bored in the blocks which required SE pressure gages. The bottoms of the holes were cleaned, and a thin coating of epoxy was placed in the center of each hole. The SE gage was gently placed on the epoxy and pressed down flush with the surface of the block. Extreme care was taken to insure that the SE gage was in full contact with the block. Figure 2.15 is an illustration of a completed SE gage installation on a block of model rock material. The completed model was lifted with an overhead crane and lowered into the test chamber (Figure 2.16). The model was then grouted into place with the same model rock material mix. Figure 2.17 is a photograph of the top surface of a model grouted in place for testing.

When construction of the model was completed, a 1/8-inch-thick, nylon-reinforced, neoprene rubber diaphragm was placed over the surface of the model and glued to the outer ring.

The piston-type lid was then lowered into place and held off the surface of the model with spacer blocks. The entire assembly was rolled into the CFS of the LBLG for testing.

2.4.4 Testing Procedure. The void between the model and the piston-type lid was filled with water, and Dynesco pressure transducers were installed to monitor the pressure. The air-to-hydraulic multiplier was connected to pressurize the chamber. All of the instrumentation was connected to signal-conditioning modules. Calibration voltages were applied to the respective FM analog tape channels, and tape deviation for each channel was adjusted to the proper level.

Calibration voltages were applied to all tape channels and recorded on magnetic tape immediately preceding the beginning of the loading cycle. Upon completion of the calibration sequence, the loading of the model surface was initiated. The loading rate was manually controlled at approximately 100 psi/min until the desired peak pressure was attained or until the surface membrane ruptured, whichever occurred first.

The data were played back and recorded on an oscillograph for

preliminary analysis of data quality.

2.4.5 Data Reduction. The analog to digital (A-D) data conversions were made on a high-speed A-D converter at a digitizing rate of 1 kHz. The digital data were then processed through a Honeywell 400 digital computer which produced magnetic plot tapes for an off-line plotter.

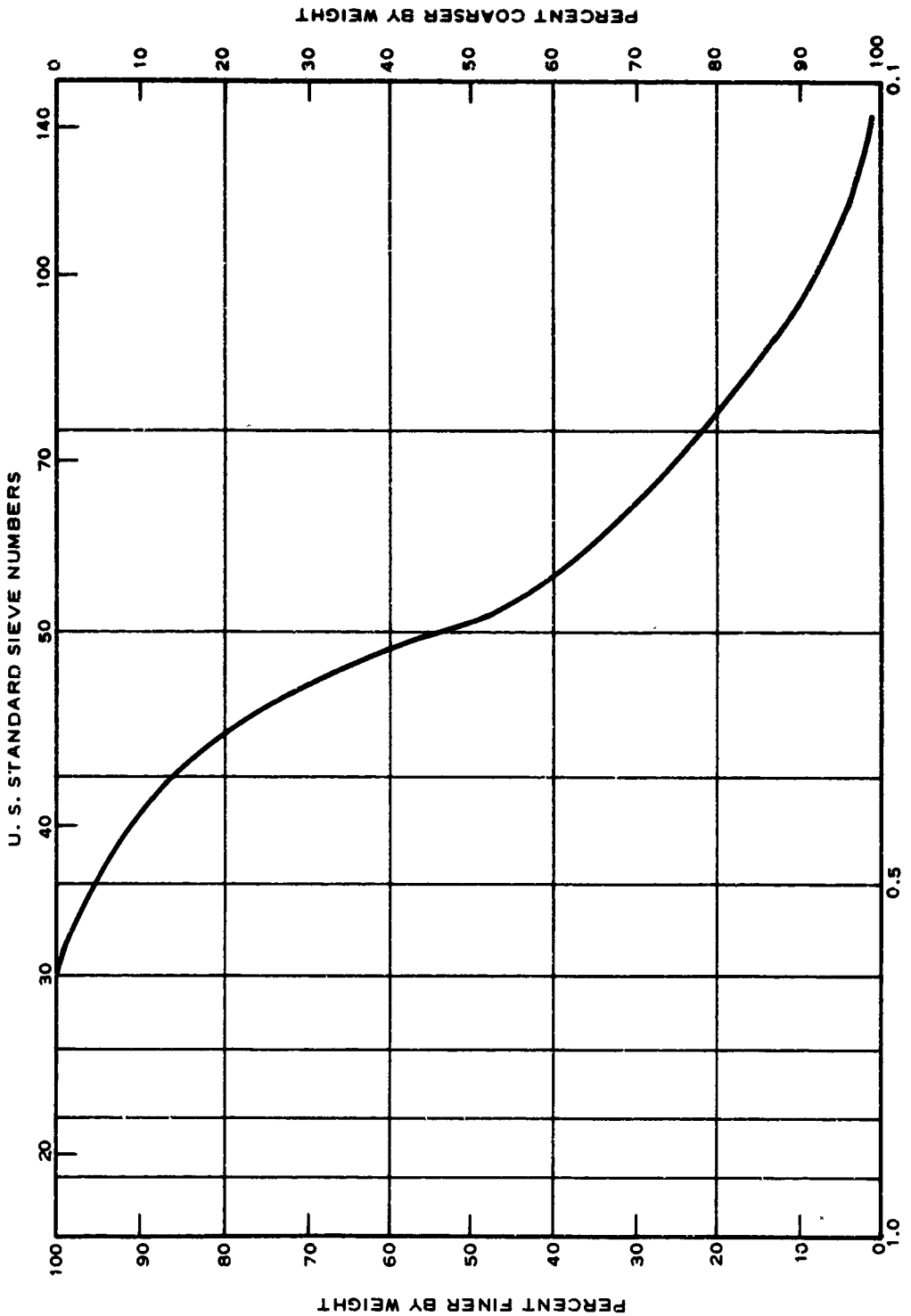

Figure 2.1 Gradation curve for sand components of model rock material.

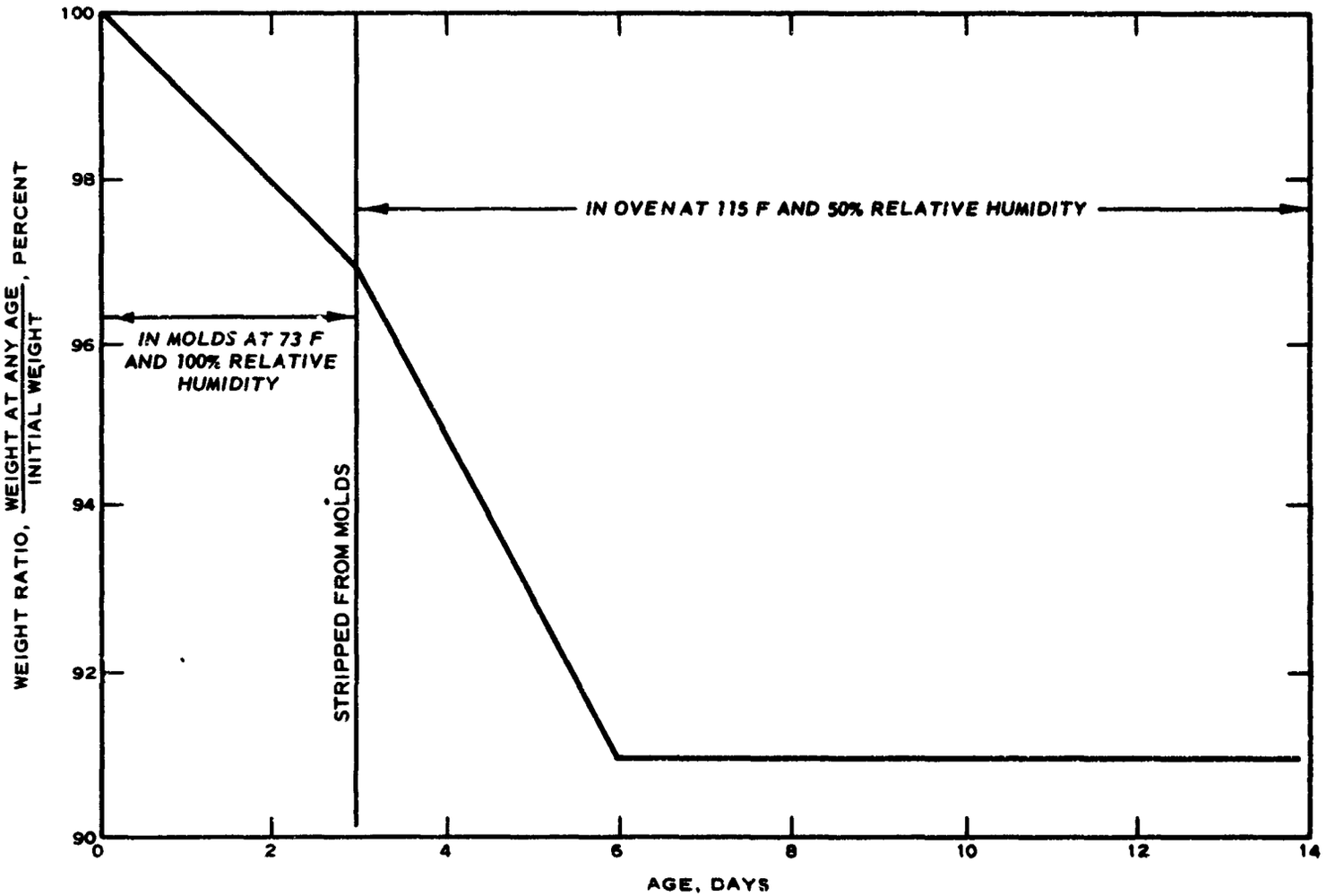

Figure 2.2 Moisture loss versus age for 3- by 6-inch cylinders of model rock material.

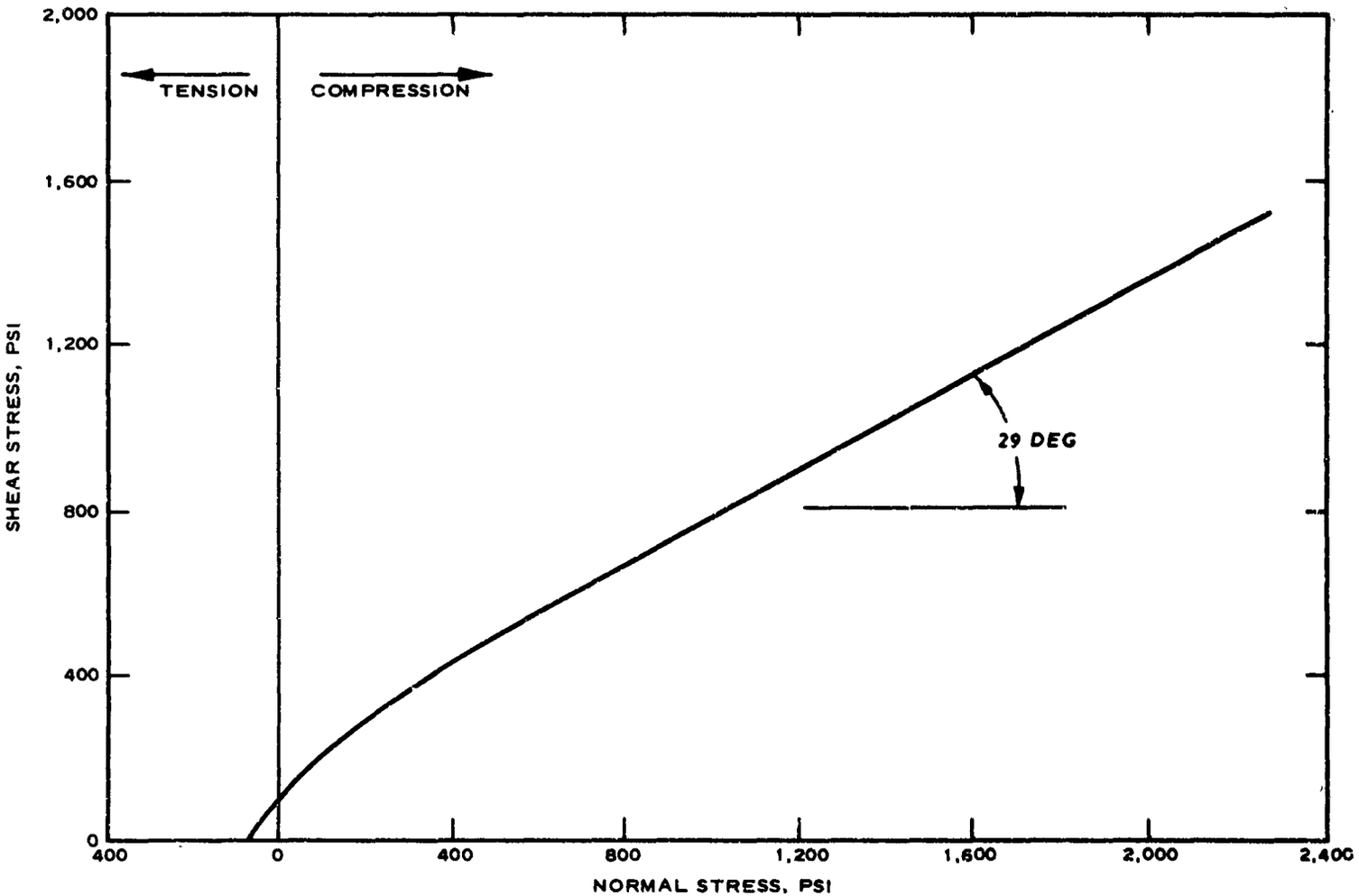

Figure 2.3 Mohr failure envelope for model rock material.

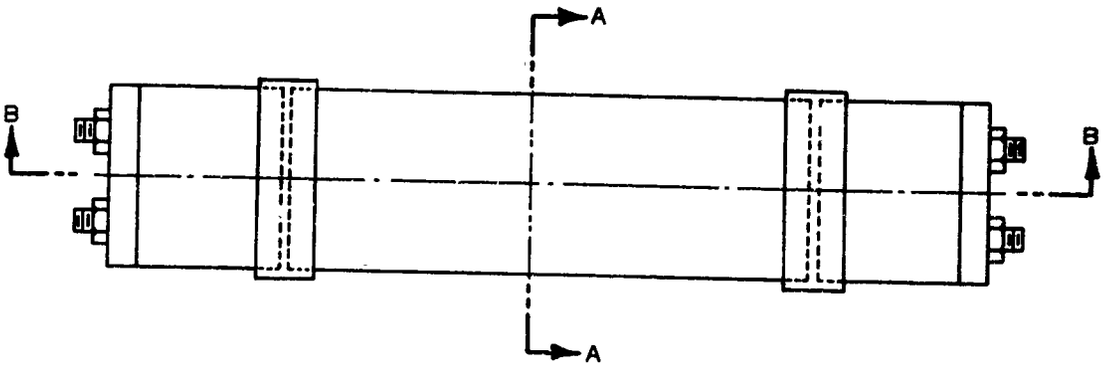

PLAN VIEW

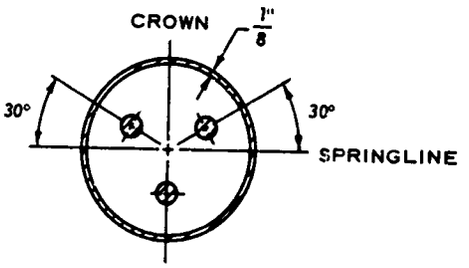

SECTION A-A

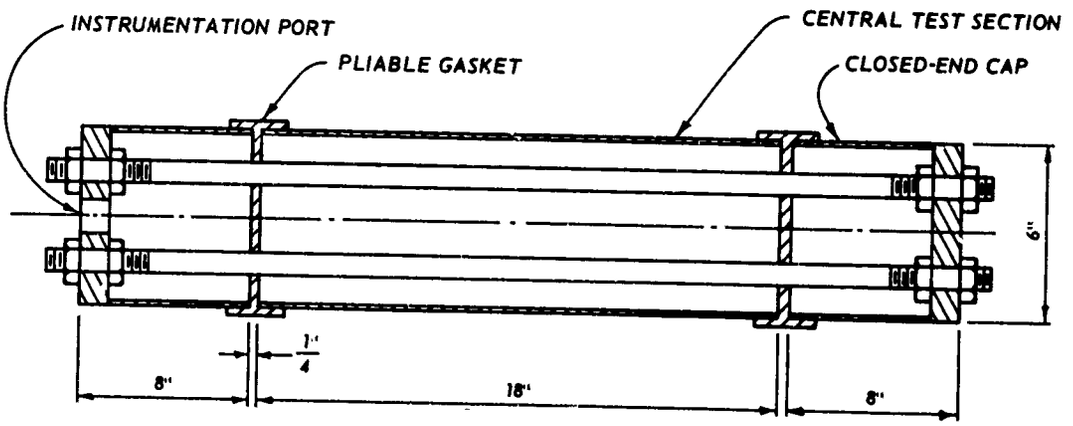

SECTION B-B

Figure 2.4 Test geometry of the cylinders.

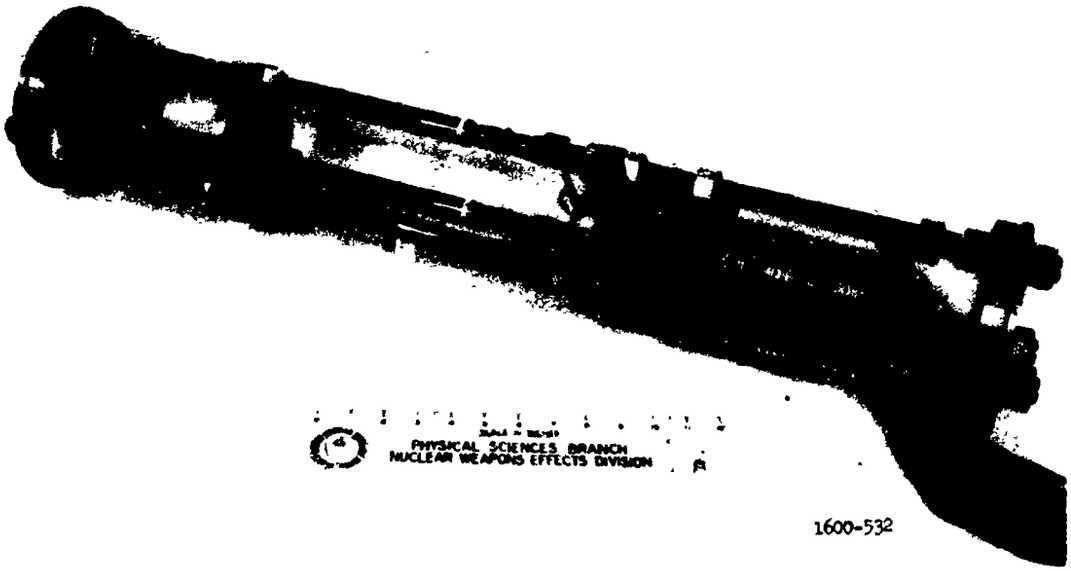

Figure 2.5 Thrust isolation assembly and dummy gage block.

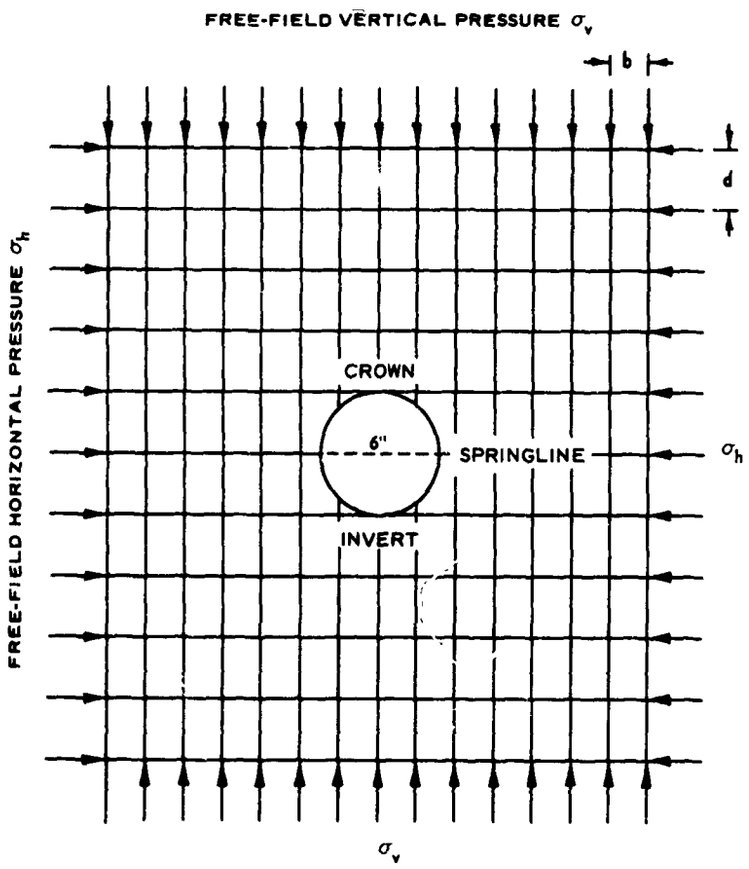

Figure 2.6 Test configuration.

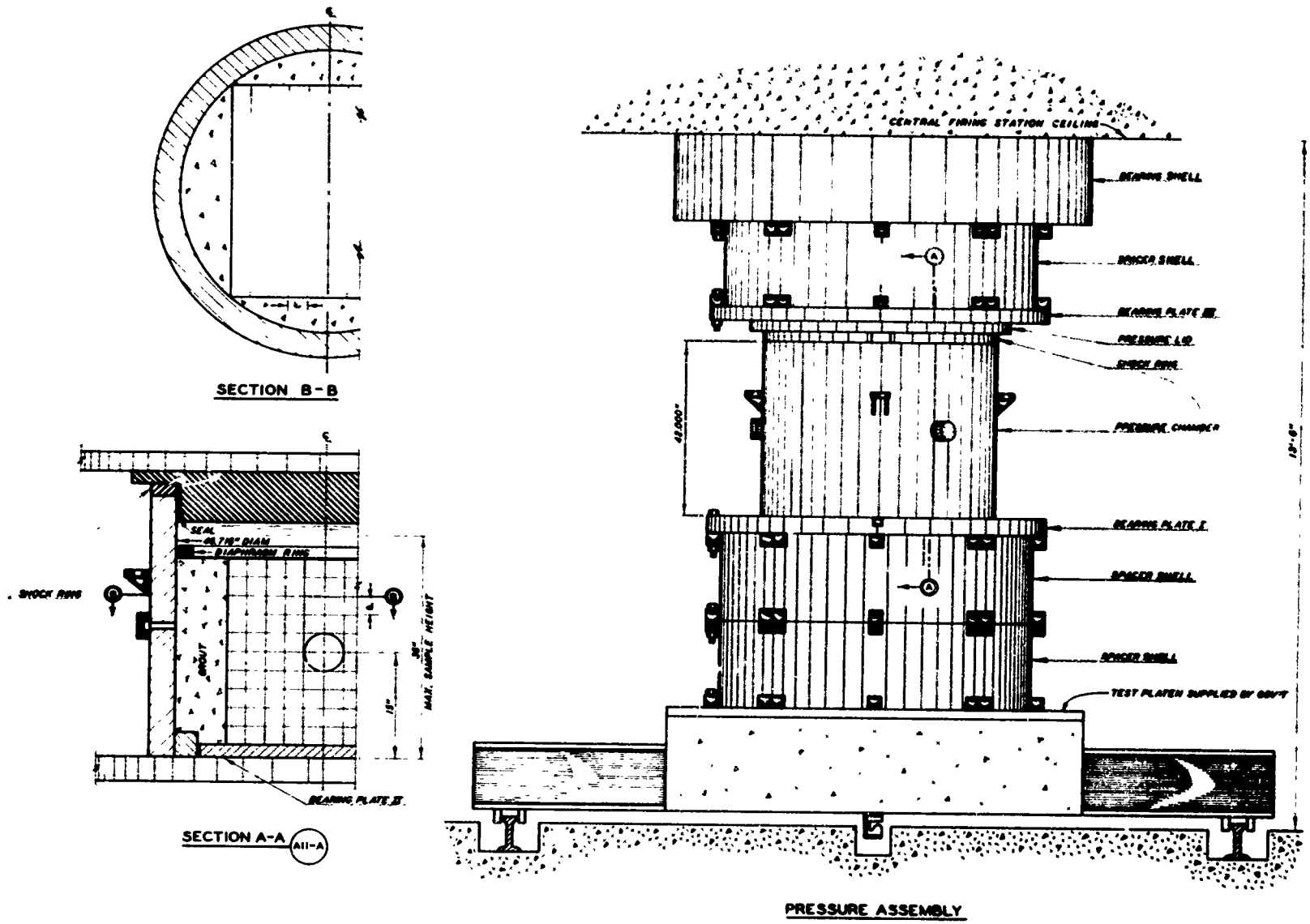

Figure 2.7 WES 6,000-psi-capacity static testing device.

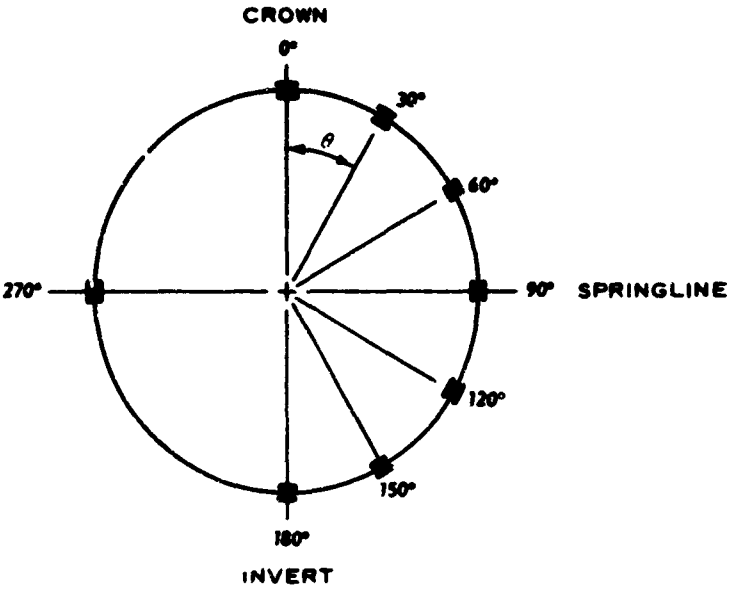

a. END VIEW OF CENTRAL TEST SECTION

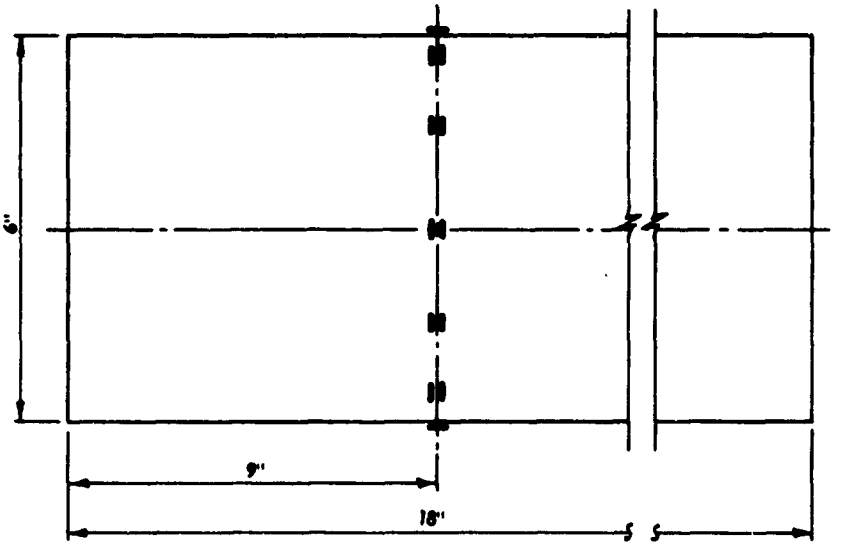

b. ELEVATION VIEW OF CENTRAL SECTION

Figure 2.8 Locations of circumferential strain gages.

Figure 2.9 Diametric extensometers in position in tunnel liner.

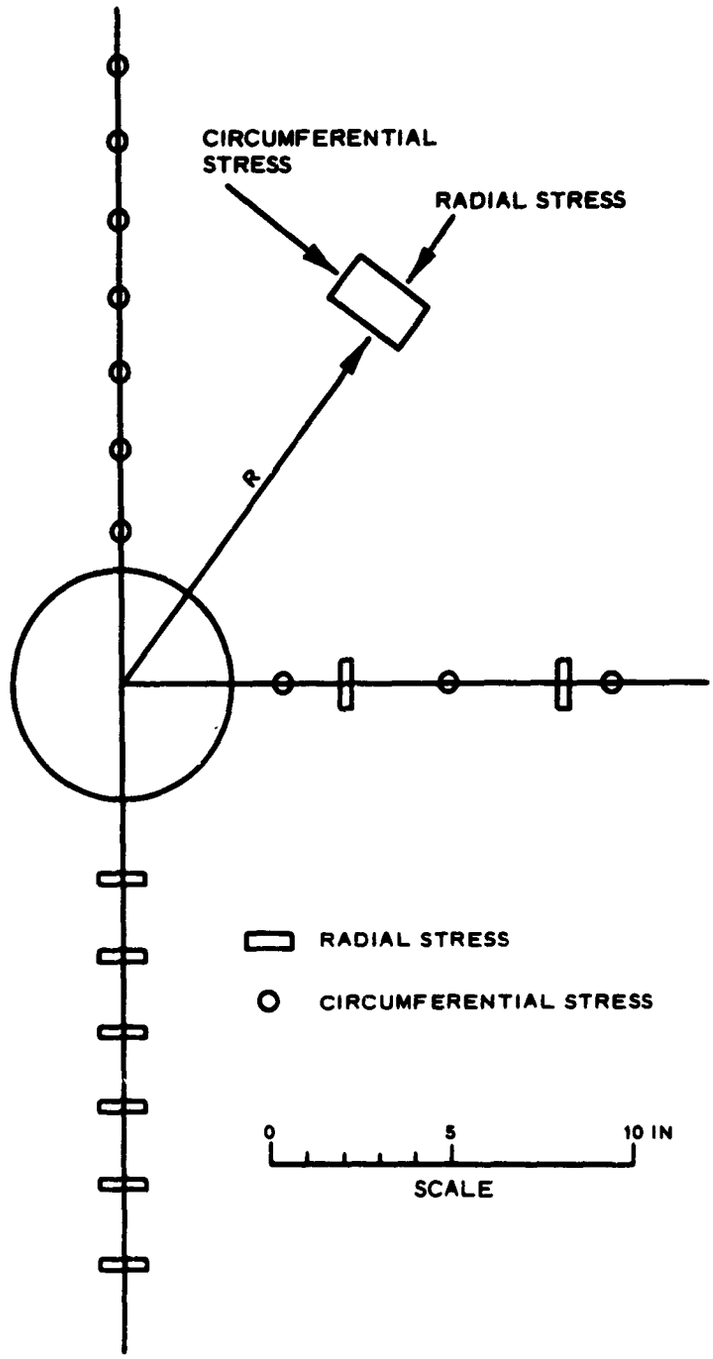

Figure 2.10 Gage layout for Model 4, b/d = 3/1 .

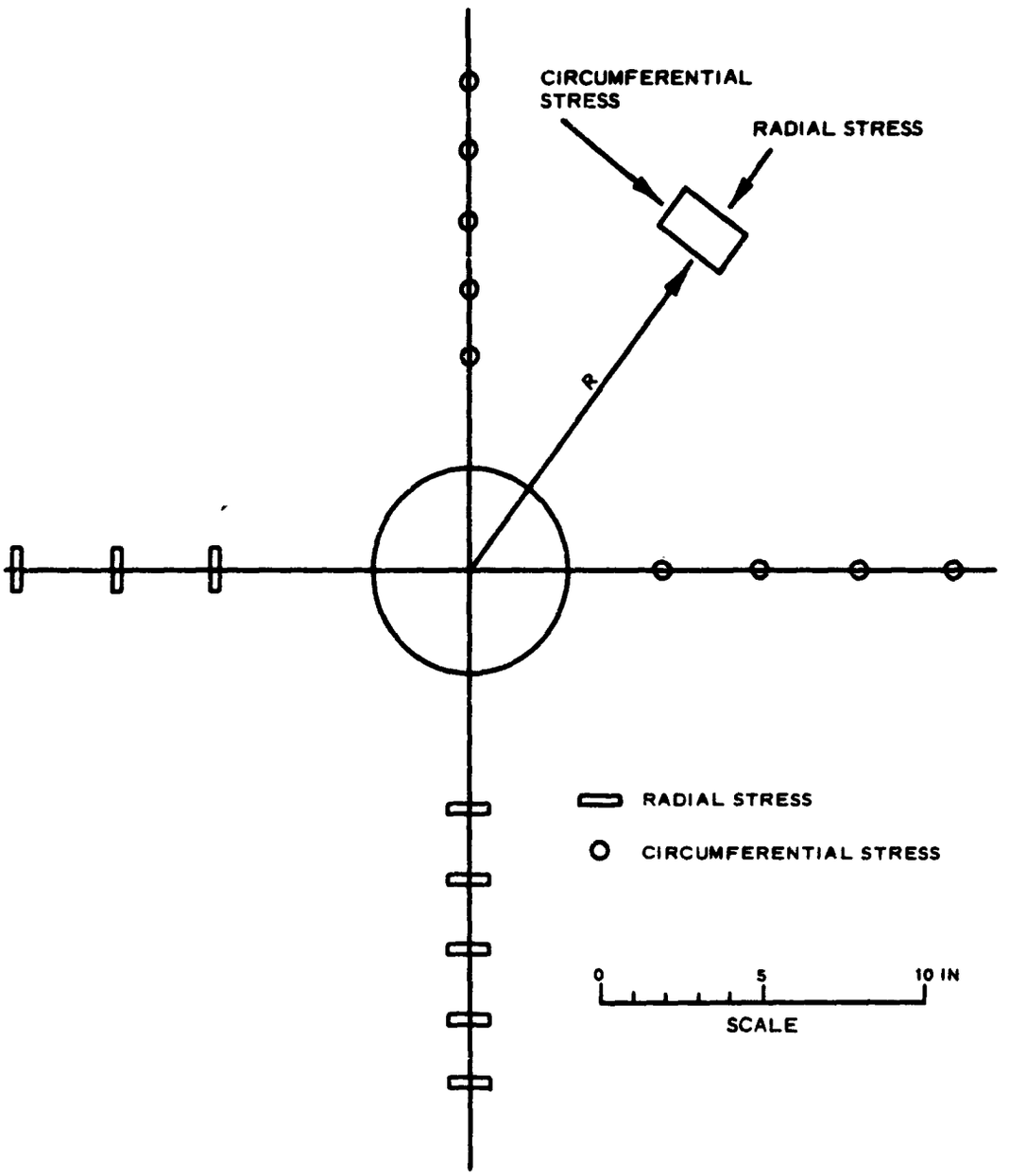

Figure 2.11 Gage layout for Model 5, b/d = 3/2 .

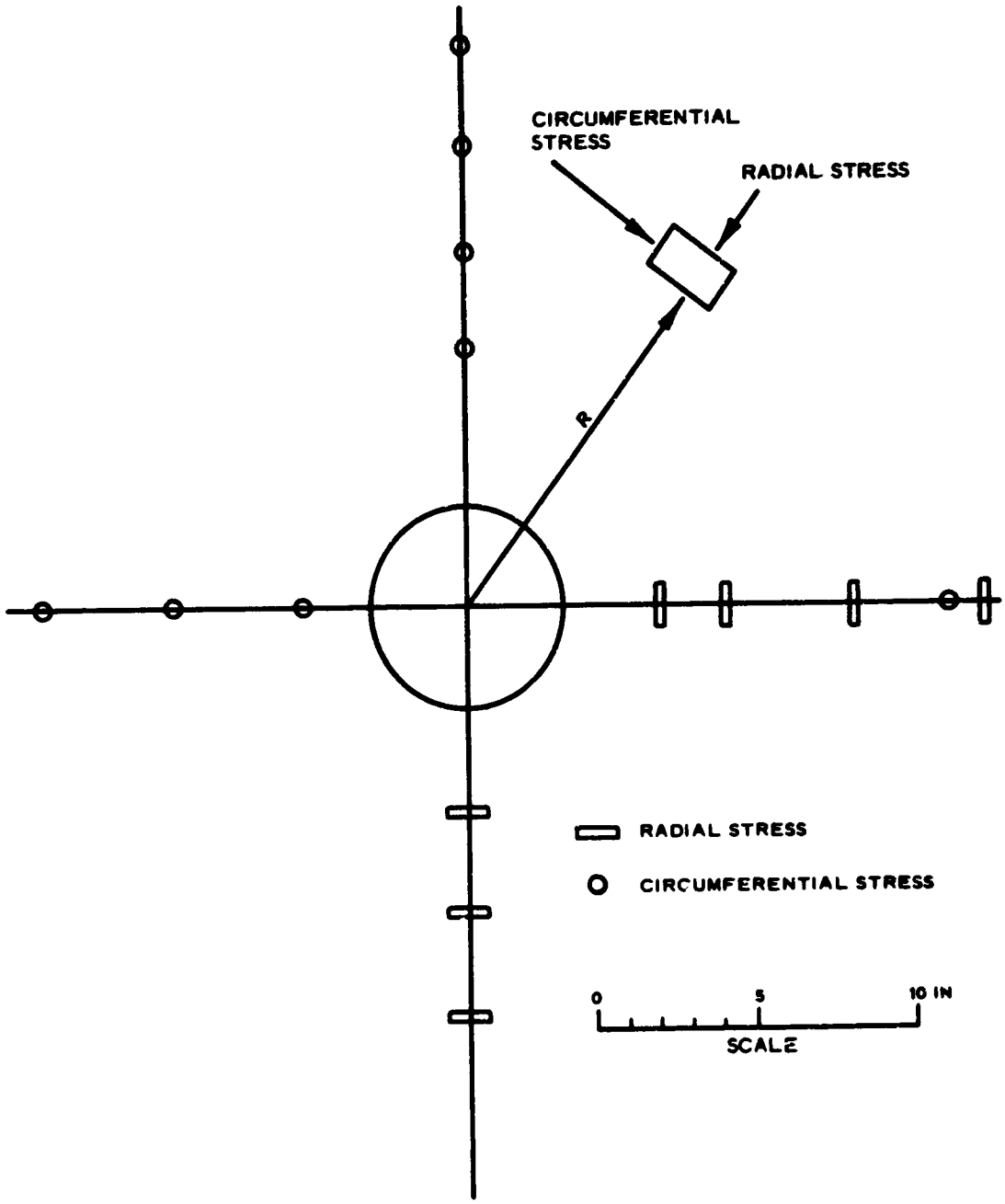

Figure 2.12 Gage layout for Model 6, $b/d = 2/3$.

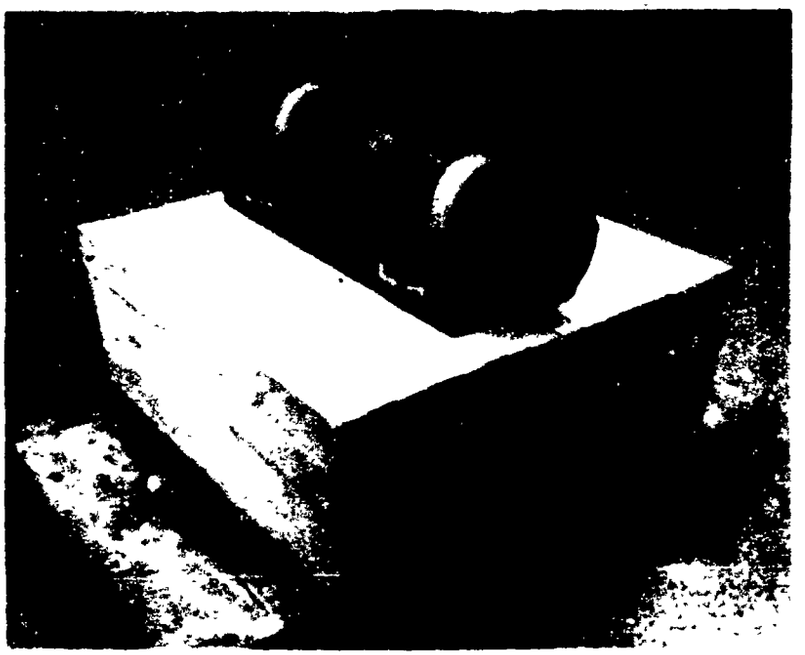

Figure 2.13 Completed cylinder assembly ready for installation.

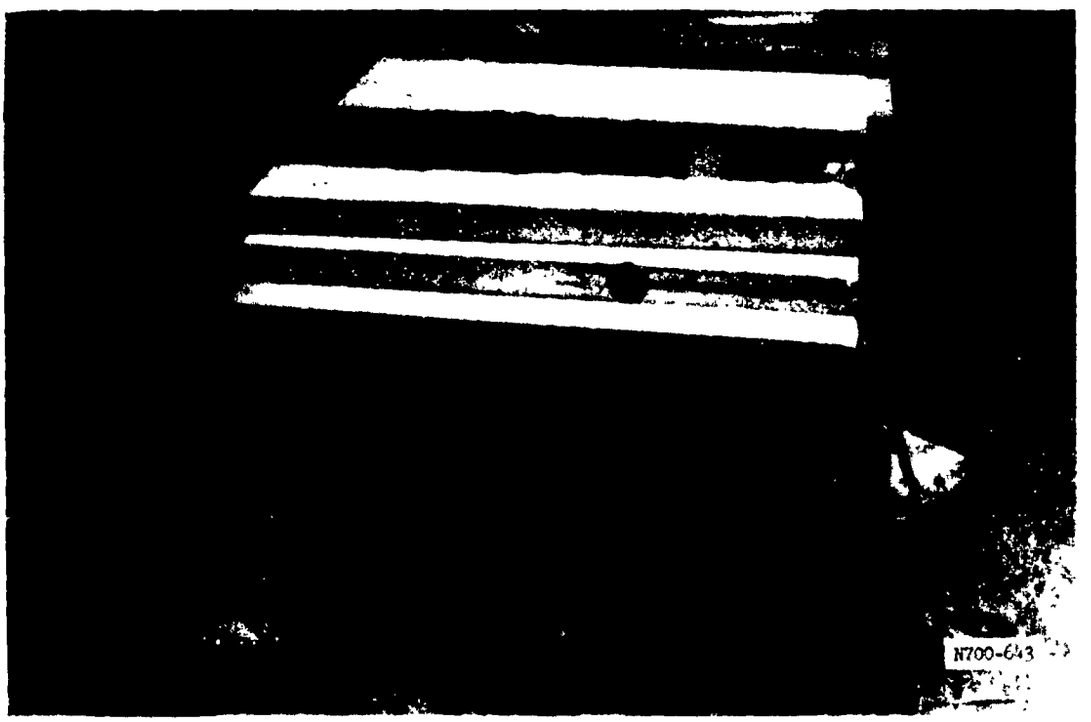

Figure 2.14 Partially assembled model rock mass.

Figure 2.15 Completed SE gage installation.

Figure 2.16 Completed model being lowered into the 6,000-psi-capacity static test device.

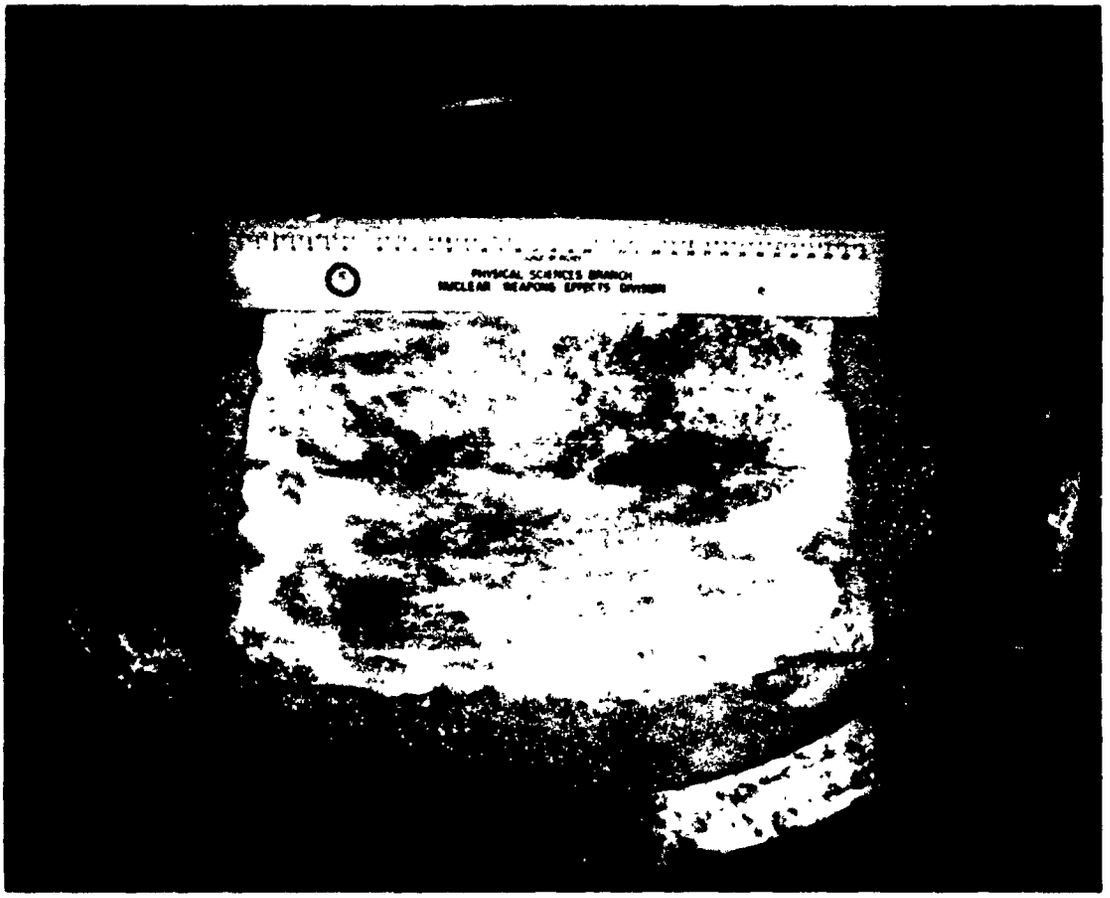

Figure 2.17 Model grouted into place for testing.

CHAPTER 3

SUMMARY OF TESTS AND PRESENTATION OF RESULTS

3.1 SUMMARY OF TESTS

A summary of the tests conducted during this study is presented in Table 3.1. Six static tests were conducted on model rock masses containing steel-lined cylindrical openings. Four tests were conducted on virgin models, and two tests were cycled loadings on the unjointed model rock mass. Reloading of the unjointed model was conducted to assess the effects that cyclic loading had on a lined opening in an unjointed medium. The unjointed model was first loaded to 500 psi and then unloaded and allowed to recover. Then the model was loaded to 1,000 psi and again allowed to recover. In the third load cycle, the load was applied until the surface membrane ruptured at approximately 2,500 psi. Statistically, the data showed that the test results could be best presented as an average for the unjointed model tests.

3.2 MOMENTS AND THRUSTS IN THE LINER

The circumferential bending moments and thrusts presented in this chapter were computed through use of the following equations by assuming linear elastic behavior of the liner.

$$M = (\epsilon_e - \epsilon_i) \frac{Et^2}{12} \tag{3.1}$$

$$T = (\epsilon_e + \epsilon_i) \frac{Et}{2} \tag{3.2}$$

Where: M = circumferential bending moment per unit length of cylinder, in-lb/in

E = Young's modulus of elasticity for the cylinder material, psi

t = wall thickness of the cylinder, inches

ϵ_e = exterior circumferential strain, in/in

ϵ_i = interior circumferential strain, in/in

T = circumferential thrust per unit length of cylinder, lb/in

Moments and thrusts causing compression in the outer fibers were considered positive.

3.3 DISCUSSION OF RESULTS

3.3.1 Thrusts. The variations of thrust with pressure at different positions in the cylinders are shown in Figures 3.1 through 3.6 for all tests. At most of the gage locations, the thrusts in the unjointed model increased linearly with increasing pressure. In general, the thrusts in the jointed models were slighly concave upward functions of the pressure. The effect of joint spacing on the thrusts, although apparently present, is statistically insignificant considering the method used to calculate the thrusts, i.e., the interior and exterior circumferential strains had opposite signs at all times and were of the same order of magnitude. These strains were algebraically subtracted in Equation 3.2, and, since they were of the same order of magnitude, they were very sensitive to the accuracy of the data.

The normalized springline thrust, T/Pa, is a measure of the active arching which occurred in all of the tests. This implies that the tunnel liners were not as stiff as the adjacent model rock masses and that a portion of the load applied over the tunnel was arched around the cylinders. Approximately 90 percent ±5 percent of the load was carried by the liners at all pressure levels in all tests.

The average of the normalized crown and invert thrusts is a measure of the lateral pressure applied to the cylinder. Figure 3.7 shows a plot of averaged normalized crown and invert thrusts as data bands.

3.3.2 Moments. The variations of the bending moments at different gage locations are shown in Figures 3.8 through 3.14. From these plots, it is apparent that jointing of rock masses has a significant effect on the moments in the liner. In general, the circumferential bending moment response is a nonlinear function of the overpressure, particularly in the low surface pressure region. As previously stated, the cylinders were less stiff than the surrounding material, and active arching developed as pressure was applied to the system. As the number of joints intersecting the cylinder increased, the stiffness of the cylinder more

closely approached the stiffness of the model rock mass, which generally resulted in a corresponding increase in the bending moments. At a surface pressure of 1,500 psi, the difference between the crown and invert bending moments for the unjointed model was 15 percent of their mean value. For the jointed models with joint spacings of 3/1, 3/2, and 2/3, the differences at 1,500-psi surface pressure were 38, 7.7, and 10 percent, respectively. Comparison of the average crown and invert bending moments with the average springline bending moments shows another trend. The ratio of the springline moments to the crown invert moments for the unjointed model was 0.54. The ratios of the springline moments for the jointed models with joint spacings of 3/1, 3/2, and 2/3 to the crown and invert mean value moments were 1.10, 0.95, and 0.98, respectively. Thus, as the relative stiffness of a cylinder increases, the springline and the average crown and invert moments become nearly equal.

3.3.3 Diameter Changes. The diameter changes of the cylinder springline and crown-invert axes with pressure are presented in Figure 3.15. The pressure required to seat the jointed models varied from approximately 100 to 300 psi.

The slope of the crown-invert curve is a measure of the effective stiffness of the model rock mass in the vertical direction. The reduction in stiffness of the models due to even widely spaced joints was very great. In the high-pressure region, after the joints had definitely closed, the slope for the unjointed model was approximately twice the slope for the jointed models. The springline diameter change curves show that the springline expanded in all cases.

3.3.4 Pressure Measurements. Average horizontal and vertical free-field pressure measurements were made at the sprirgline axis of the model. Figure 3.16 presents a plot of horizontal free-field pressure versus vertical surface pressure. The curves were essentially linear and the ratios of horizontal to vertical pressure for the unjointed model and jointed models were 1/2 and 1/1, respectively. Figure 3.17 shows the radial pressure distribution across the springline axis for the jointed models. As the number of joints increased, the ratio of radial pressure to surface pressure increased near the liner; however, the free-field

radial pressure was essentially the same for all of the jointed models. The normalized circumferential pressures are plotted as a data band in Figure 3.18.

TABLE 3.1 SUMMARY OF TESTS CONDUCTED

Test Number	Tunnel Diameter	Joint Spacing		Remarks
		Horizontal	Vertical	
	inches	inches	inches	
1	6	No joints	4-inch epoxied jcint	First loading of specimen
2	6	No joints	4-inch epoxied joint	Second loading of specimen
3	6	No joints	4-inch epoxied joint	Third loading of specimen
4	6	6	2	b/d = 3/1
5	6	3	2	b/d = 3/2
6	6	2	3	b/d = 2/3

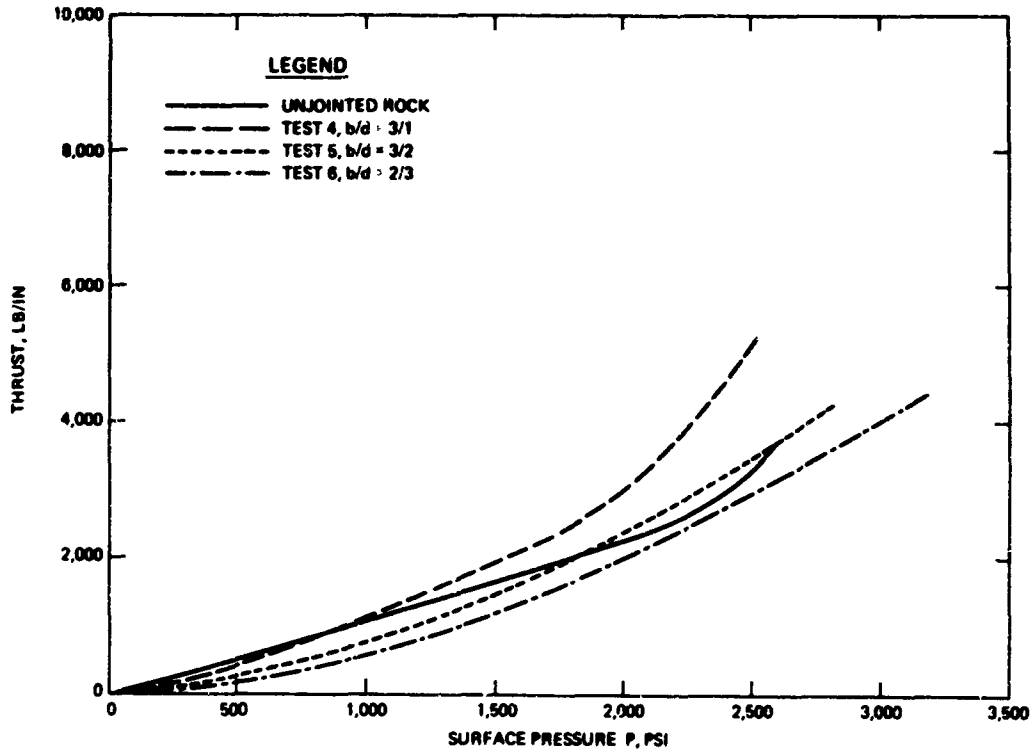

Figure 3.1 Thrust versus surface pressure at crown, θ = 0 deg.

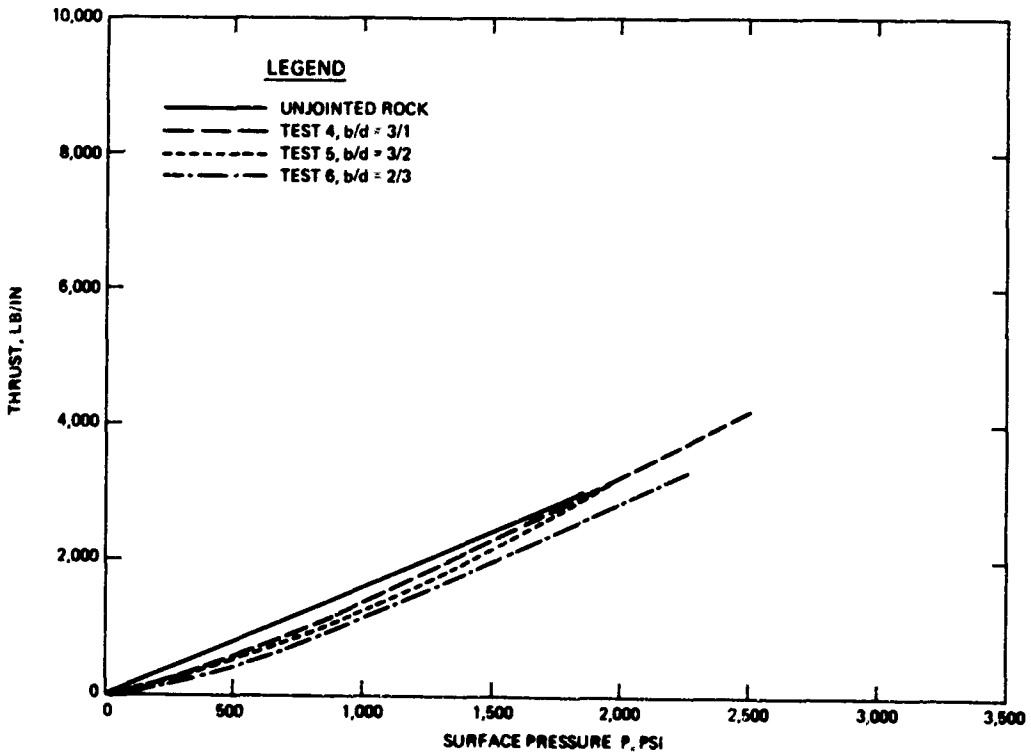

Figure 3.2 Thrust versus surface pressure at θ = 30 deg.

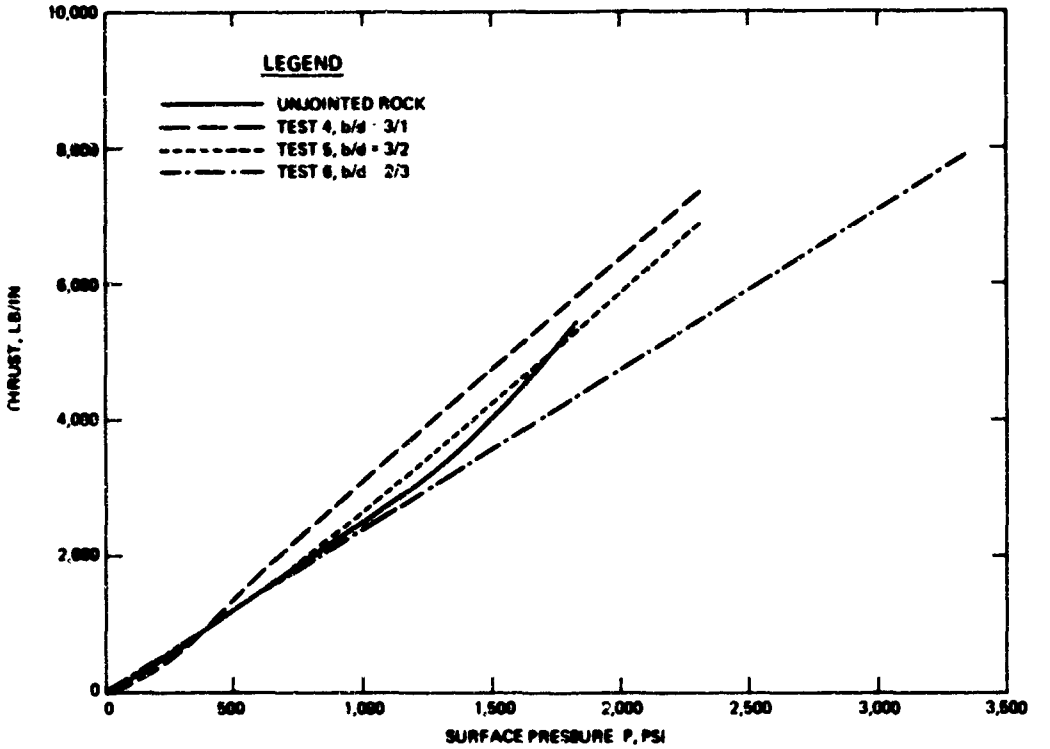

Figure 3.3 Thrust versus surface pressure at springline, θ = 90 deg.

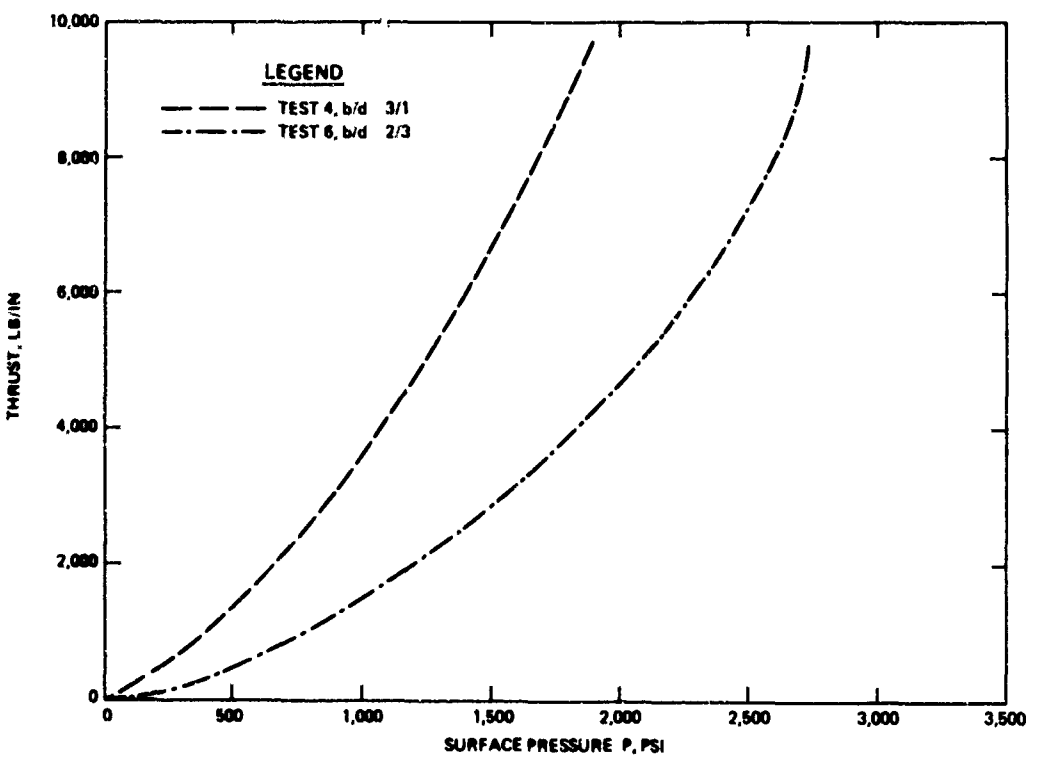

Figure 3.4 Thrust versus surface pressure at θ = 120 deg.

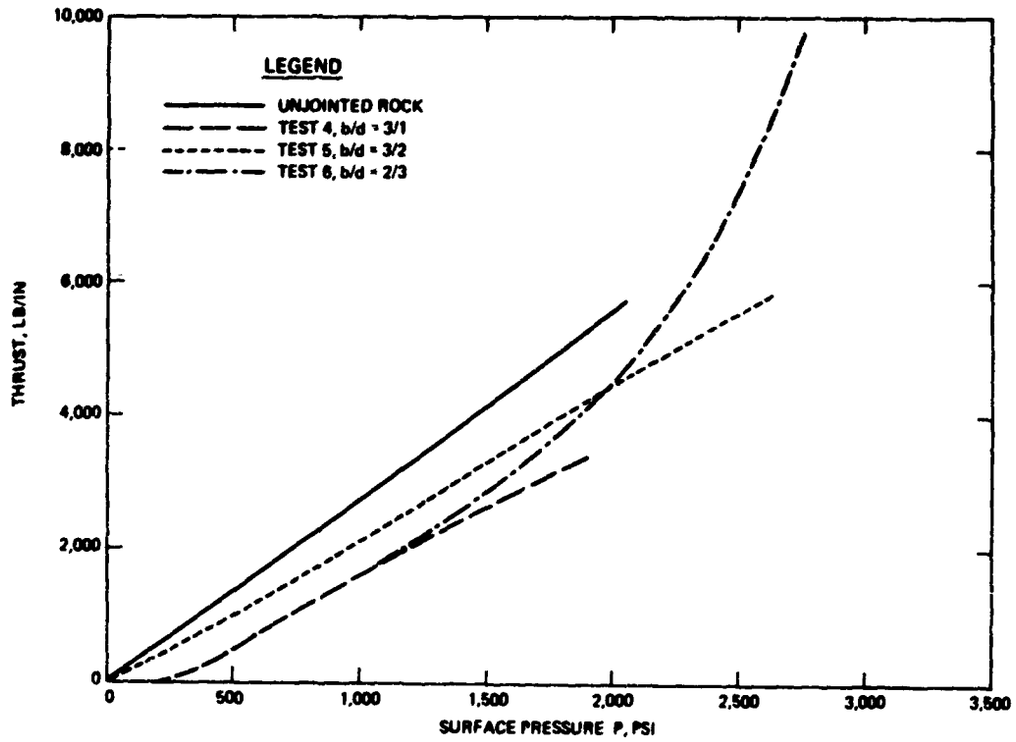

Figure 3.5 Thrust versus surface pressure at θ = 150 deg.

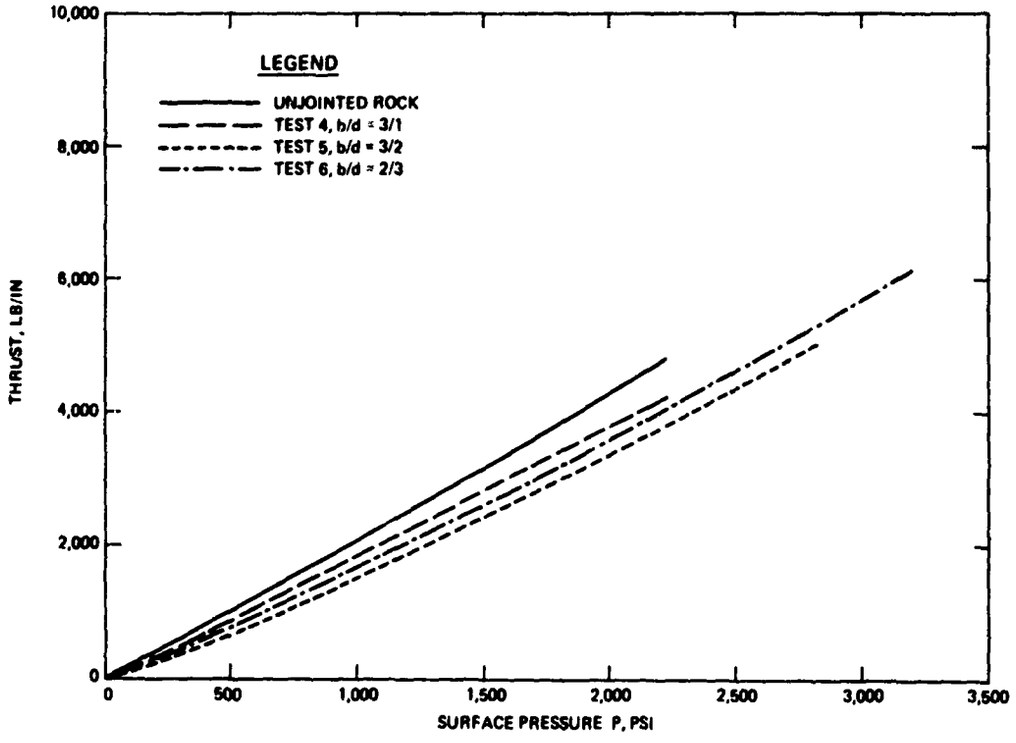

Figure 3.6 Thrust versus surface pressure at invert, θ = 180 deg.

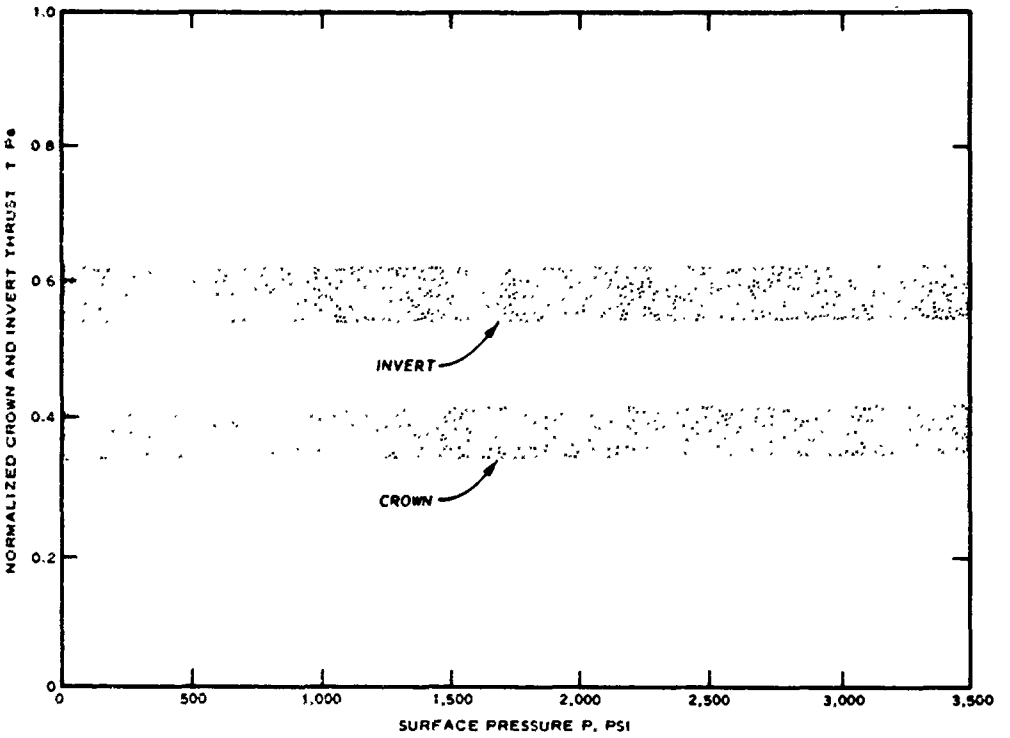

Figure 3.7 Normalized crown and invert thrusts versus surface pressure.

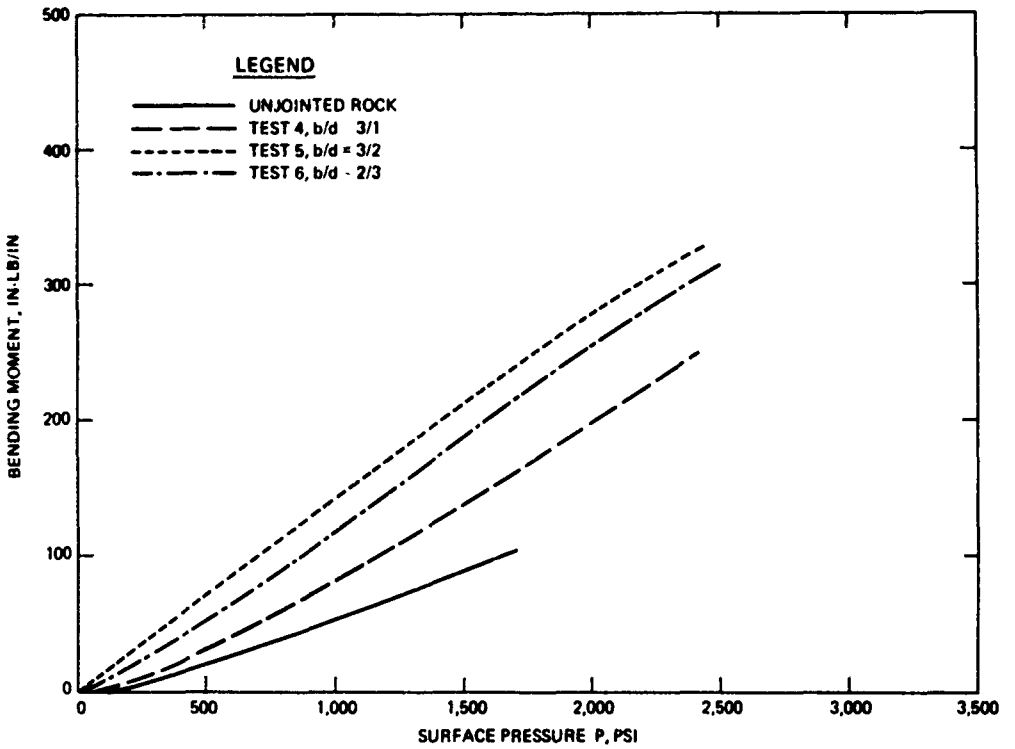

Figure 3.8 Bending moment versus surface pressure at crown, $\theta = 0$ deg.

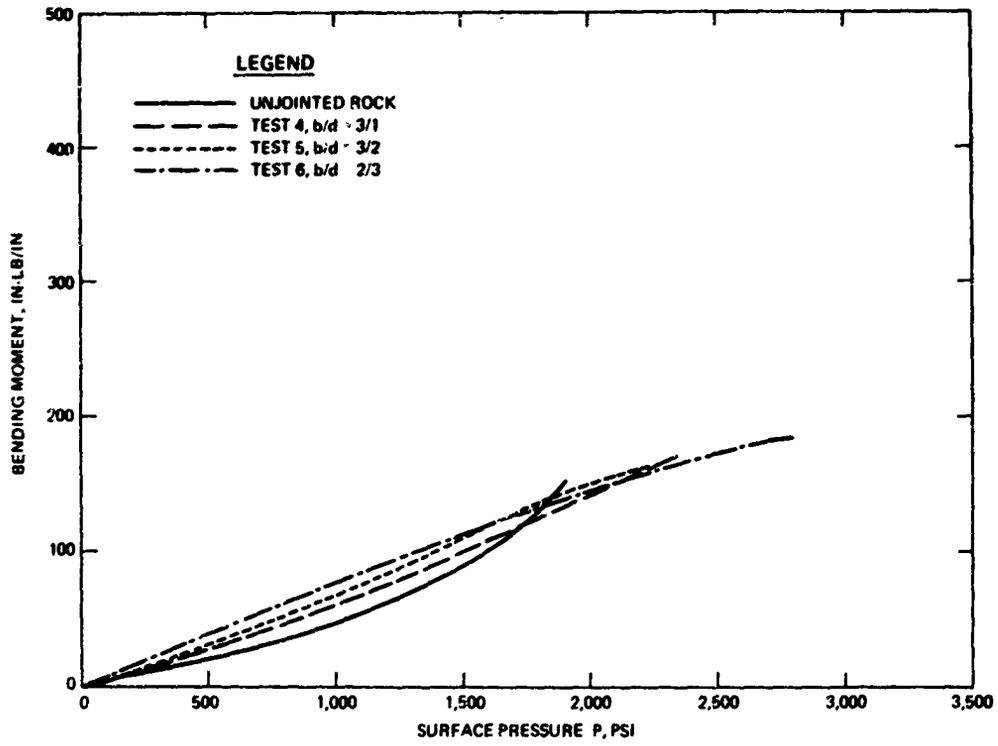

Figure 3.9 Bending moment versus surface pressure at θ = 30 deg.

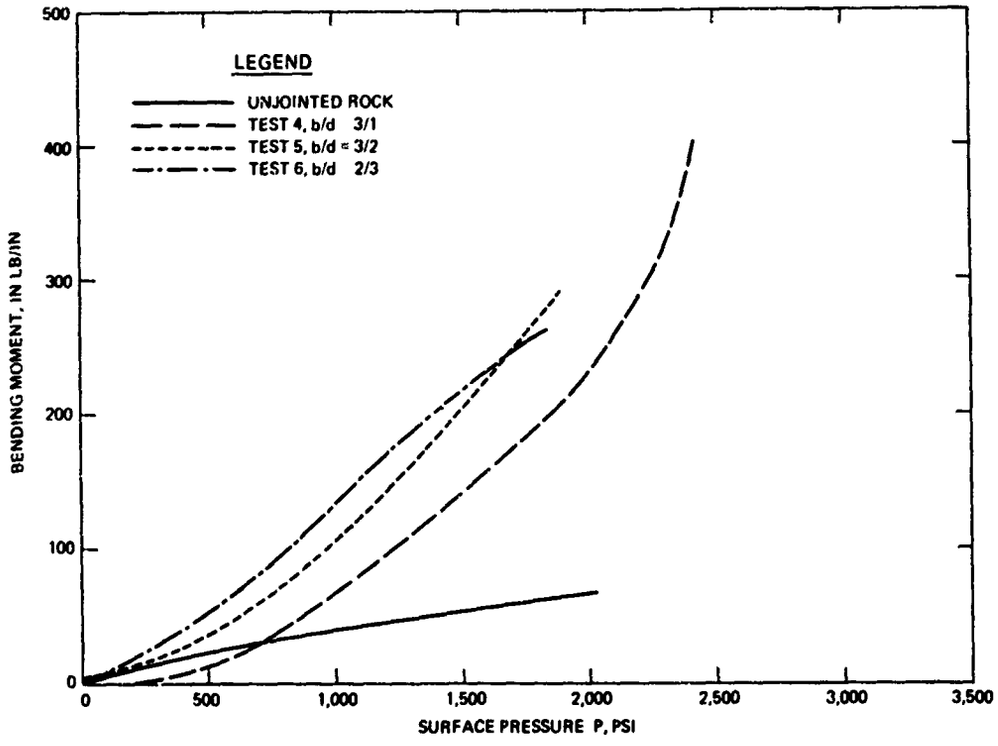

Figure 3.10 Bending moment versus surface pressure at springline, θ = 90 deg.

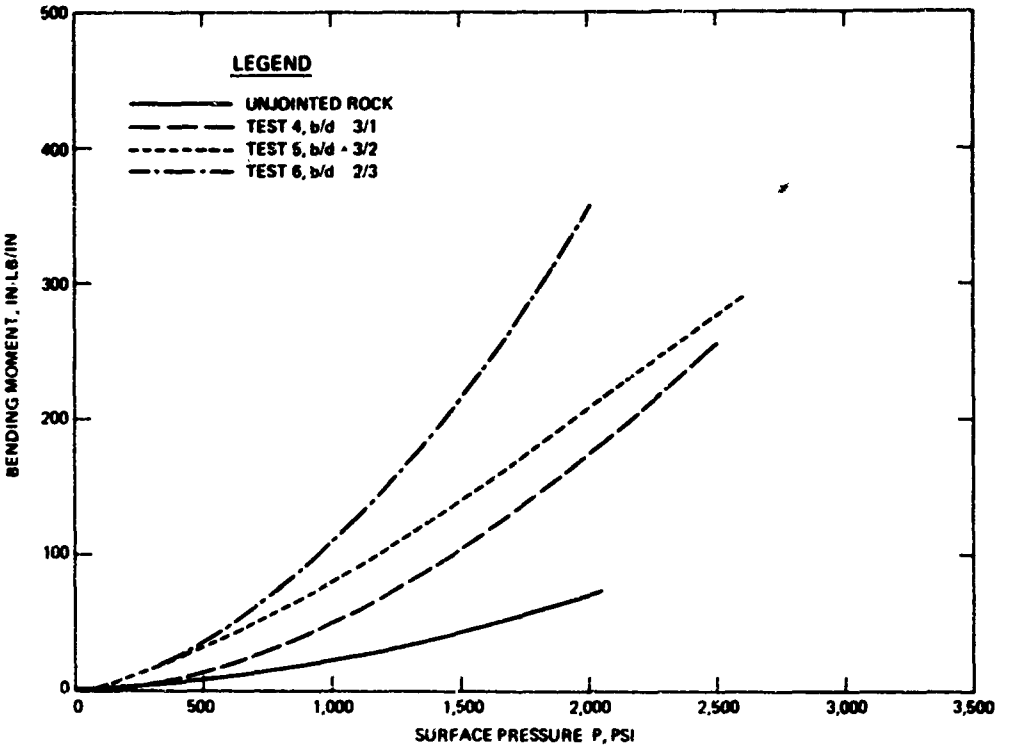

Figure 3.11 Bending moment versus surface pressure at θ = 120 deg.

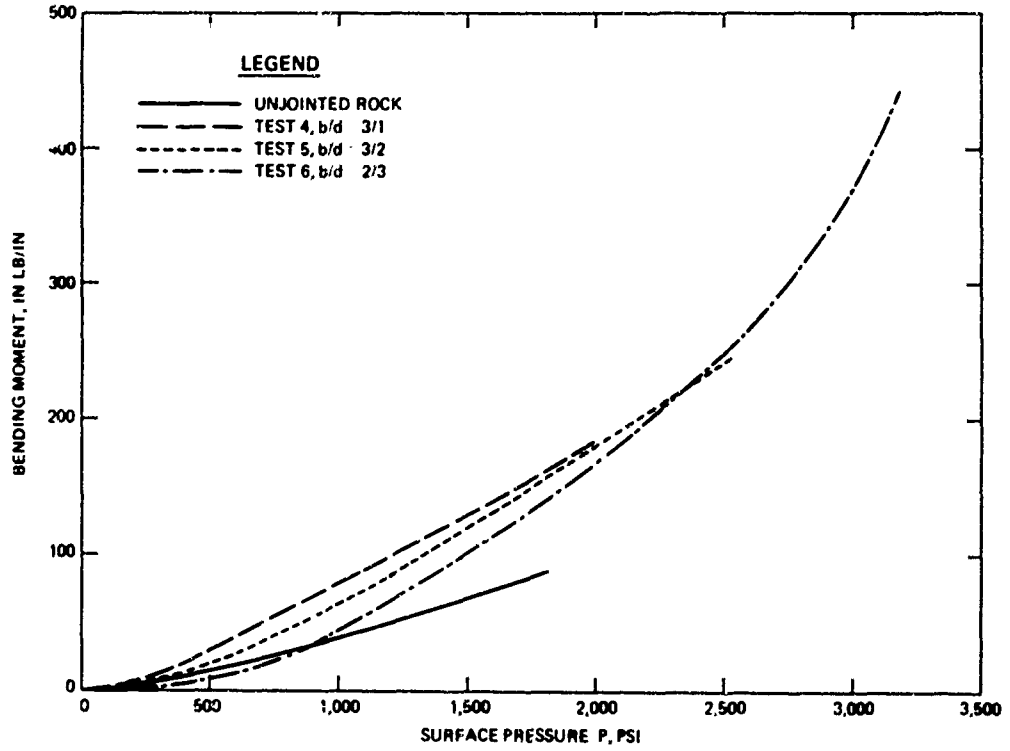

Figure 3.12 Bending moment versus surface pressure at θ = 150 deg.

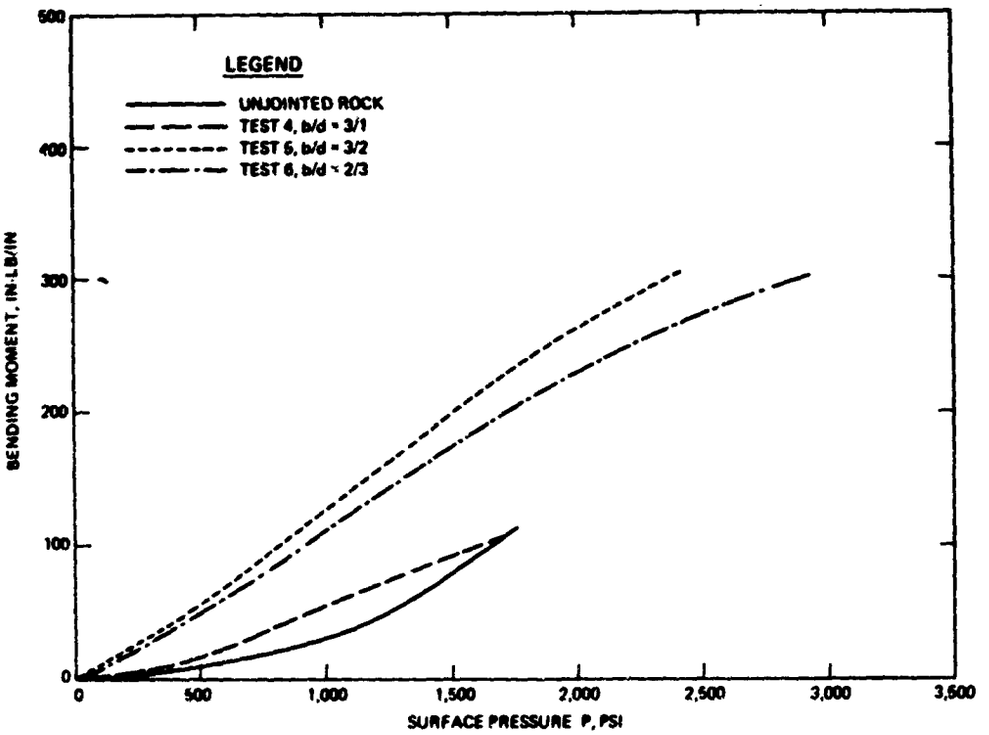

Figure 3.13 Bending moment versus surface pressure at invert, θ = 180 deg.

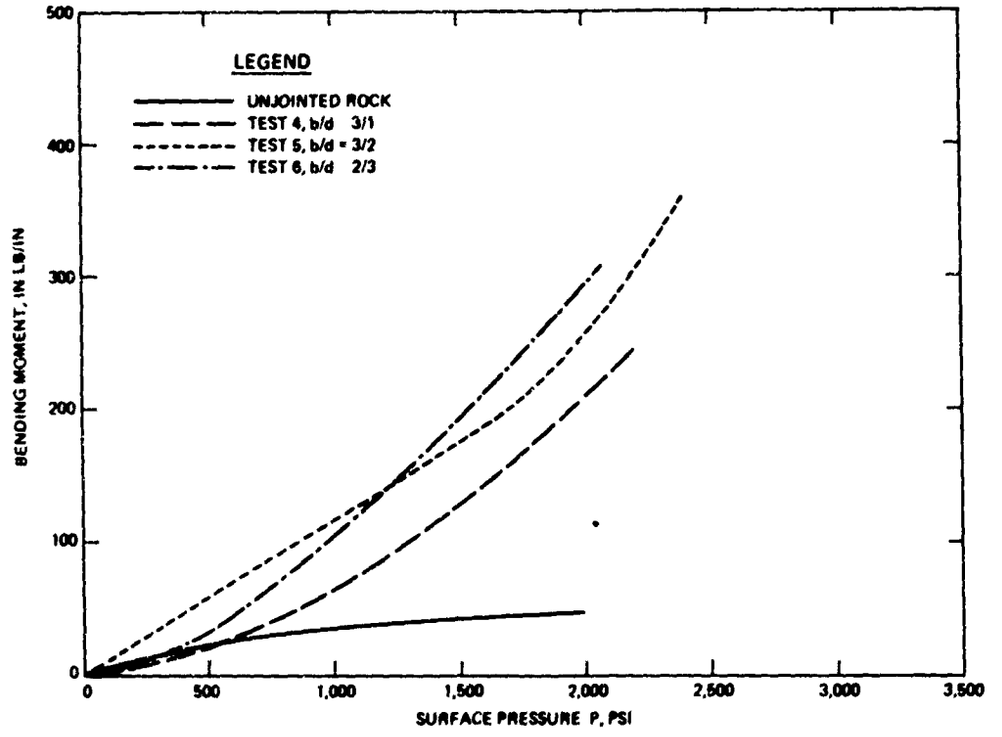

Figure 3.14 Bending moment versus surface pressure at springline, θ = 270 deg.

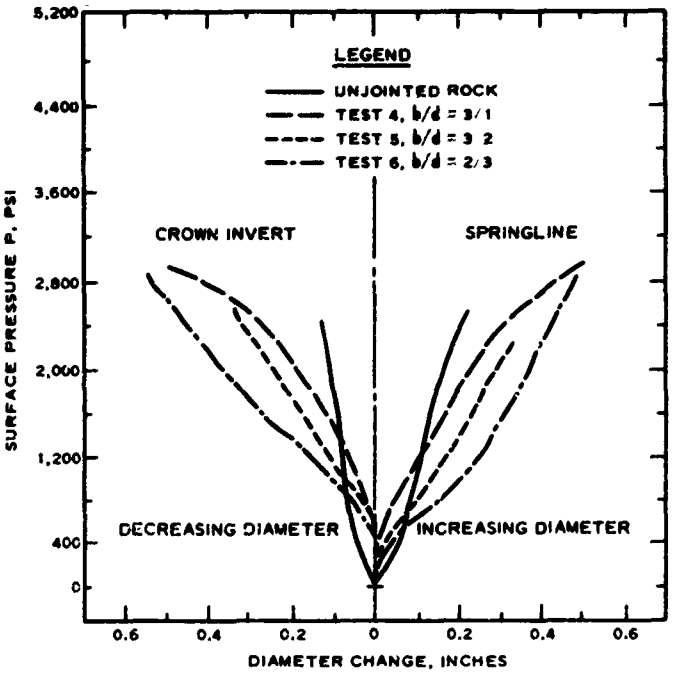

Figure 3.15 Diameter change versus surface pressure.

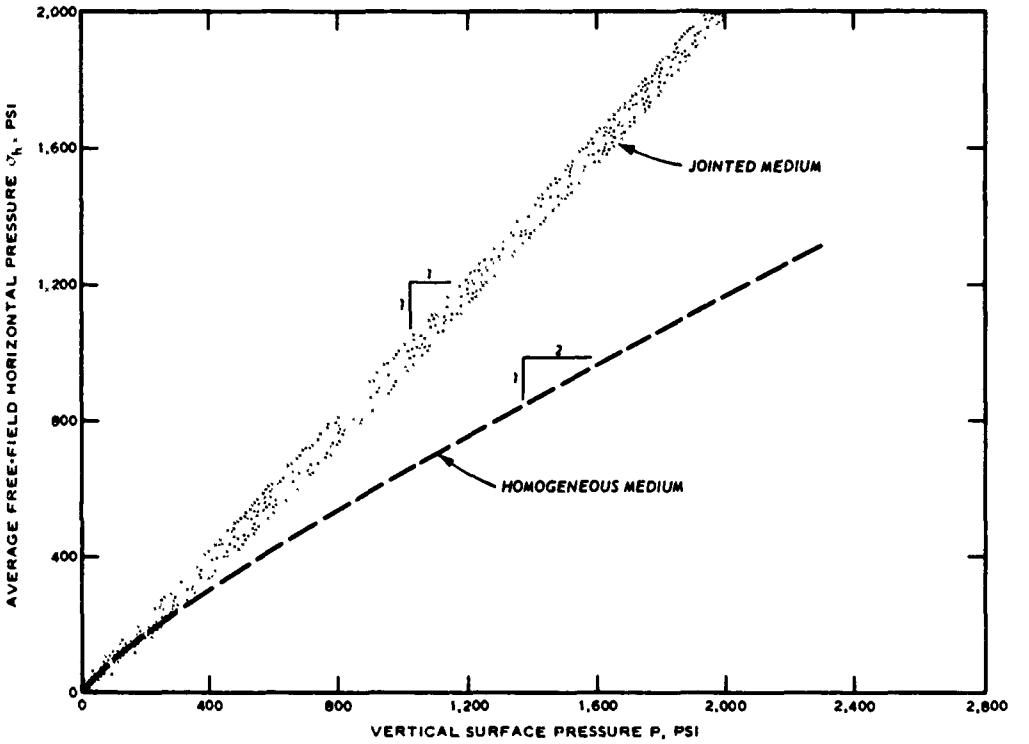

Figure 3.16 Average free-field horizontal pressure versus surface pressure.

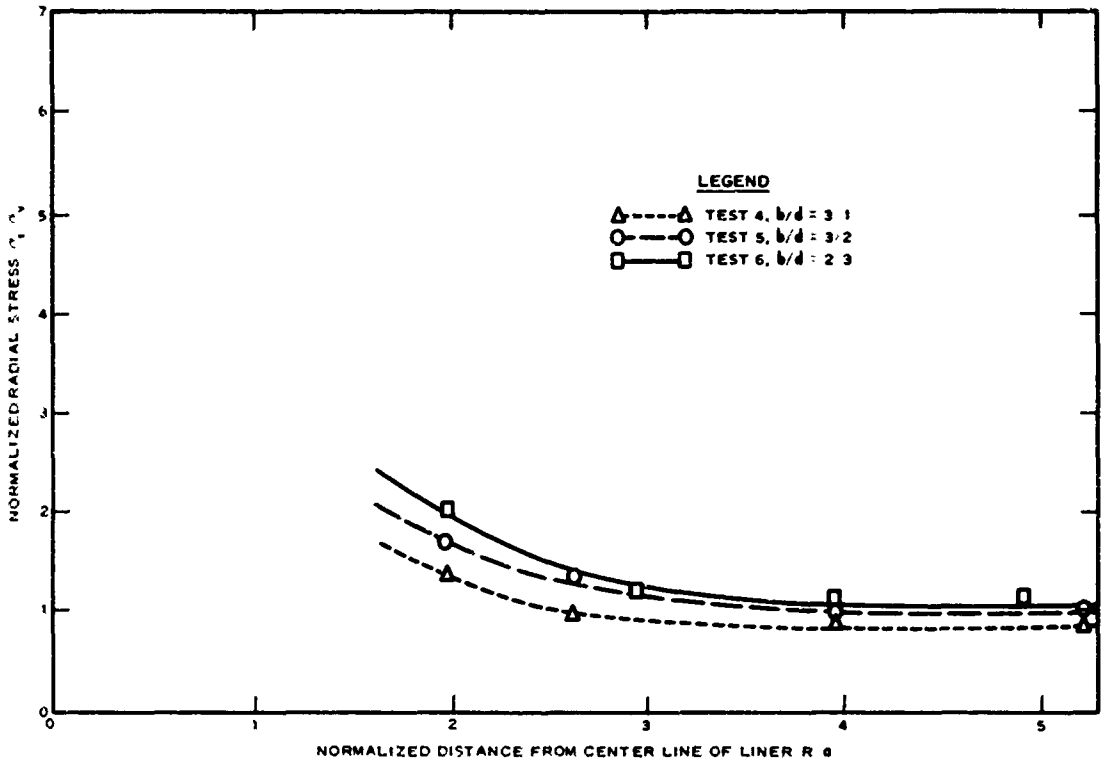

Figure 3.17 Radial stress distribution for the jointed models at the springline.

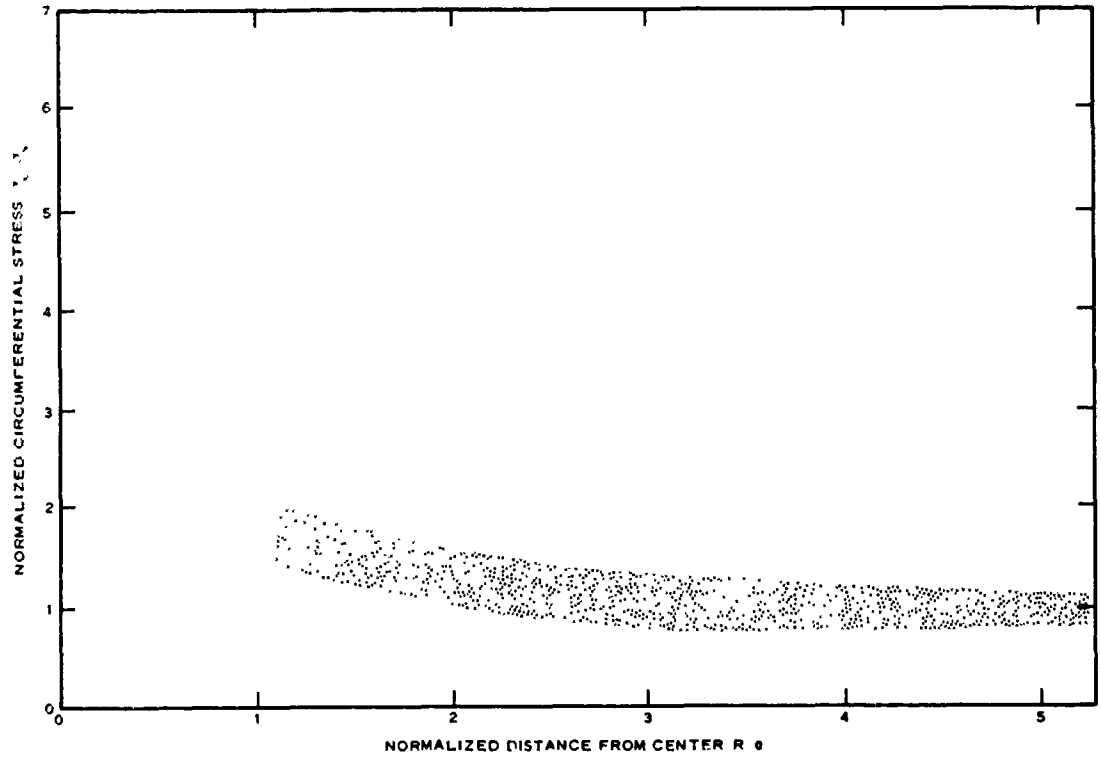

Figure 3.18 Normalized circumferential stress distribution for the jointed models at the springline.

CHAPTER 4

CONCLUSIONS AND RECOMMENDATIONS

4.1 CONCLUSIONS

4.1.1 Cylinder Thrusts. The cylinder thrusts were generally a linear function of the applied overpressure. As expected, the maximum thrust occurred at the springline, and the minimum thrust occurred at the crown and invert. The decrease of model stiffness due to jointing did not noticeably affect the thrust. Approximately 90 percent ±5 percent of the applied overpressure was carried by the liners, which is indicative of active arching. This implies that the cylinders were not as stiff as the adjacent model rock material.

4.1.2 Cylinder Moments. The circumferential bending moments in the cylinders were nonlinear functions of the overpressure and, in general, increased at an increasing rate with applied pressure. The maximum moments occurred at the crown, invert, and springline and were approximately of the same order of magnitude. The maximum moments in the jointed models were 3 to 5 times the maximum moments in the unjointed model.

4.1.3 Diameter Changes. A popular belief is that the stiffness modulus of a jointed rock mass is reduced by the separation of the joints but that after the joints close the stiffness will approach that of an unjointed rock mass. However, in these model rock tests the stiffness was drastically reduced even by widely spaced joints at high overpressures.

In general, the stiffness moduli of the jointed rock mass model did not show any tendency to increase with applied overpressure. The average stiffness of the unjointed model was approximately twice that of the jointed rock models. Within the data spread in these tests, the influence of joint spacing on stiffness was not obvious.

4.1.4 Pressures. The ratio of the free-field horizontal to vertical pressure in the jointed rock models approached a common value of one, while the ratio for the unjointed rock model was approximately one-half.

Increasing the number of joints increased the ratio of radial pressure to overpressure near the liner at the springline.

4.1.5 Joint Spacing Effects. The influence of joint spacing on the response of the system can be summarized as follows:

1. The stiffness moduli of the jointed models approach a common value at high pressures, but an increase in the number of joints increases the diameter change significantly.

2. The ratio of horizontal to vertical free-field pressure in the jointed model rock approaches a common value of one irrespective of the joint frequency.

3. The radial stress at the springline shows a significant increase near the liner as the number of joints increases.

The circumferential stress distribution appeared to be independent of joint spacing.

4.2 RECOMMENDATIONS

The experimental program should be continued to determine the dynamic response of the cylinders. These tests could be conducted in the WES 1,500-psi-capacity Shock Tube Facility. It would be desirable to test modeled reinforced concrete liners in order to obtain insight into the effects of material properties on the mode of failure.

Analytical studies using the finite element method should be coordinated with the experimental study in order to develop prediction capabilities. The analytical approach should include the nonlinear behavior of the system as well as the static and dynamic responses.

APPENDIX A

MODEL ROCK PROPERTIES

The model rock material used throughout this study was adapted from the model material developed by Rosenblad (Reference 6). Static unconfined and triaxial tests were conducted on 3- by 6-inch cylindrical specimens to determine the stress-strain characteristics of the material developed at WES, which was modeled after Rosenblad's material. The results of these tests are presented in Figures A.1 through A.3.

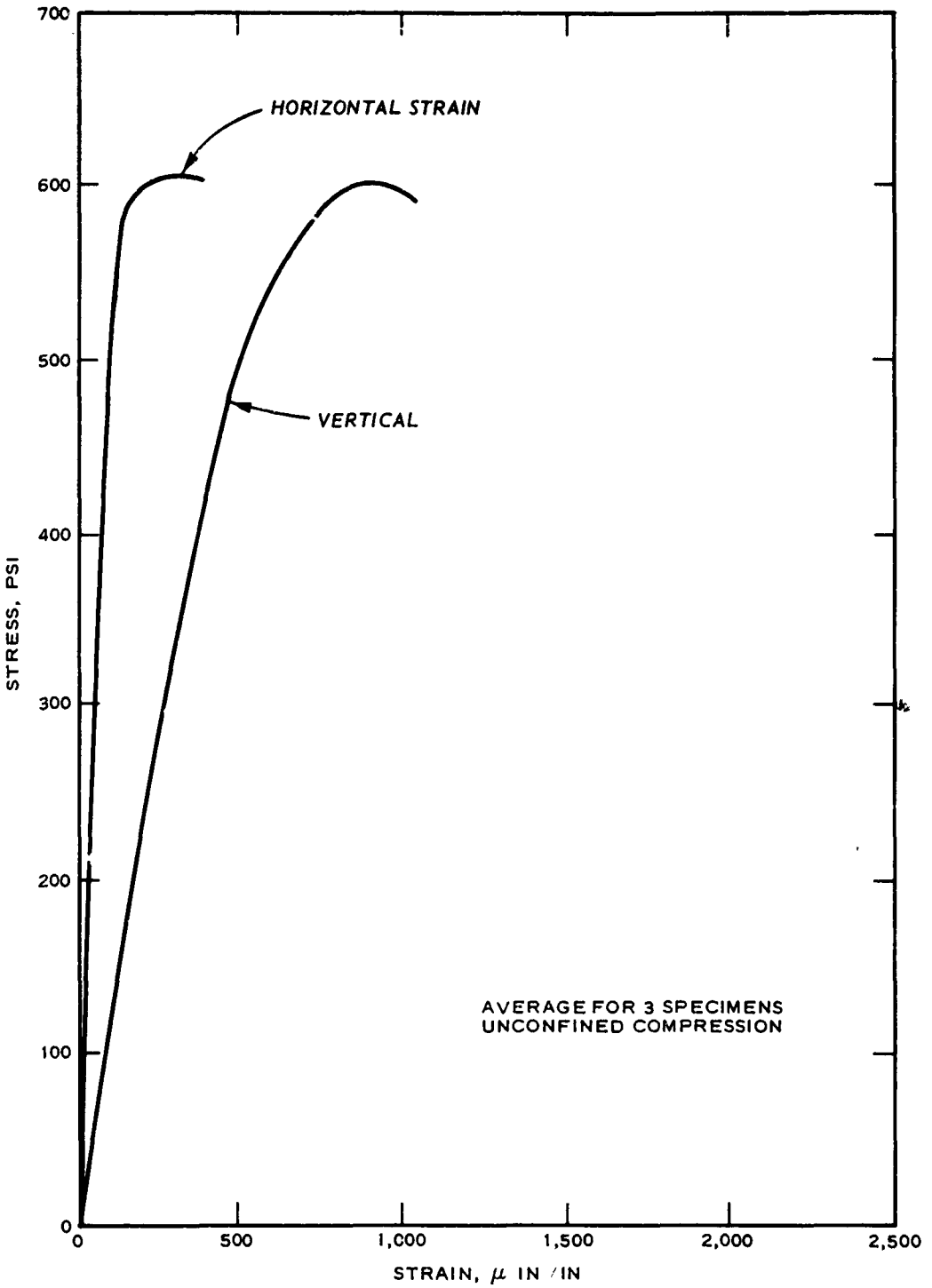

Figure A.1 Average unconfined stress-strain curves.

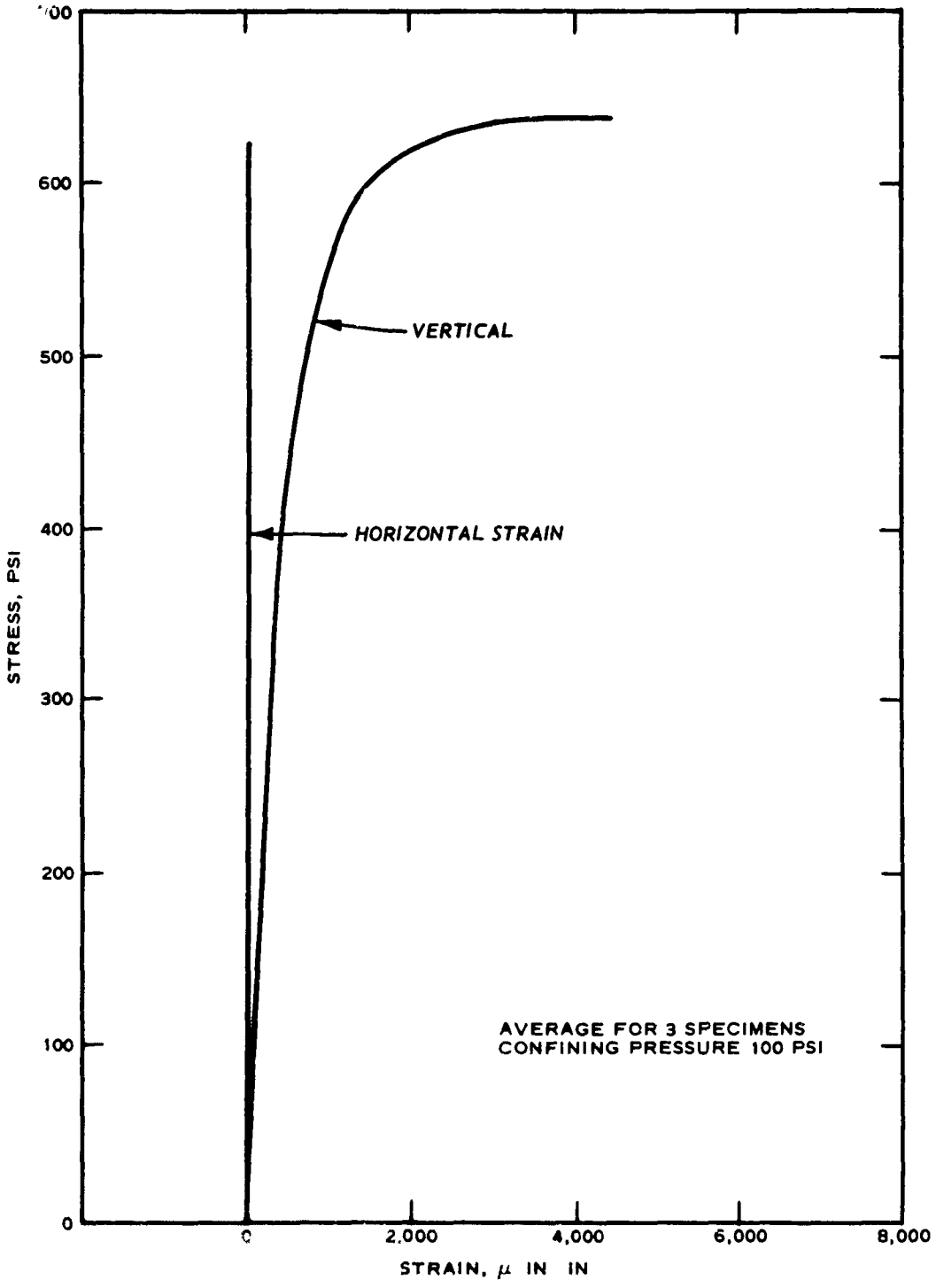

Figure A.2 Average triaxial stress-strain curves for a confining pressure of 100 psi.

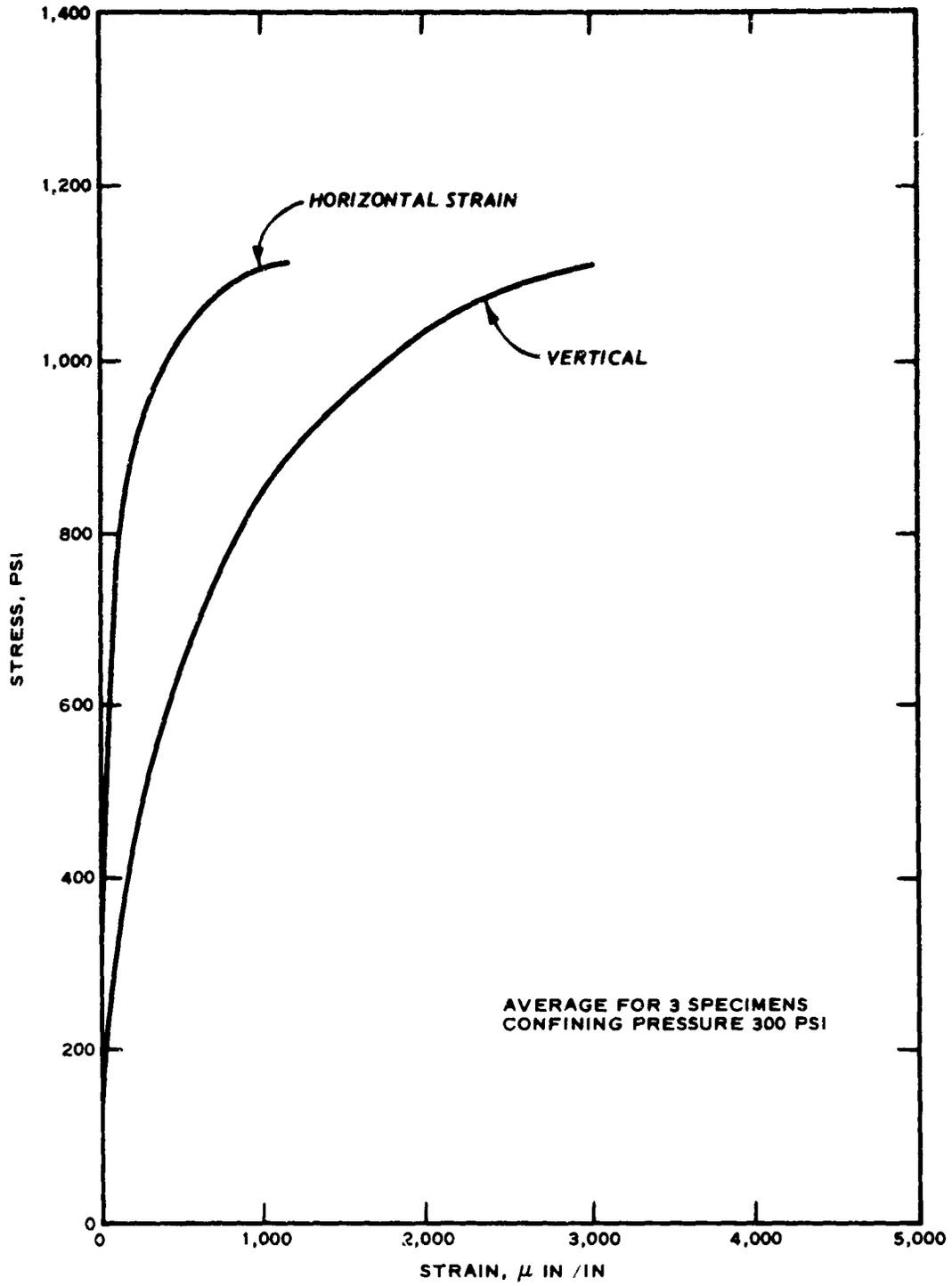

Figure A.3 Average triaxial stress-strain curves for a confining pressure of 300 psi.

REFERENCES

1. K. Barron and G. Larocque; "Development of a Model for a Mine Structure"; Proceedings, Rock Mechanics Symposium, McGill University, Montreal, Canada, 7-8 September 1962; Pages 145-190; Unclassified.

2. G. Everling; "Model Tests Concerning the Interaction of Ground and Roof Support in Gate-Roads"; International Journal of Rock Mechanics and Mining Sciences, 1964, Vol. 1, Pages 319-326; Pergamon Press, Oxford, England; Unclassified.

3. E. Hoek; "Rock Fracture Under Static Stress Conditions"; CSIR Report MEG 383, October 1965; Council for Scientific and Industrial Research, National Mechanical Engineering Research Institute, Pretoria, South Africa; Unclassified.

4. D. W. Hobbs; "Scale Model Studies of Strata Movement Around Mine Roadways, Apparatus, Technique and Some Preliminary Results"; International Journal of Rock Mechanics and Mining Sciences, 1966, Vol. 3, No. 2, Pages 101-128; Pergamon Press, Oxford, England; Unclassified.

5. E. Fumagalli; "Communication Sur Les Matériaux Pour Modèles Statiques de Barrages en Béton (Study on Appropriate Materials for Static and Dynamic Tests on Models)"; Fifth International Congress on Large Dams, Paris, Vol. IV, 1955, Copy 26, Pages 1039-1074; Unclassified.

6. J. L. Rosenblad; "Geomechanical Model Study of the Failure Modes of Jointed Rock Masses"; Technical Report MRDL 1-71, January 1971; U. S. Army Engineer Division Laboratory, Missouri River, Omaha, Nebraska; Unclassified.

7. R. E. Heuer and A. J. Hendron, Jr.; "Geomechanical Model Study of the Behavior of Underground Openings in Rock Subjected to Static Loads; Tests on Unlined Openings in Intact Rock"; Contract Report N-69-1, Report 2, February 1971; U. S. Army Engineer Waterways Experiment Station, CE, Vicksburg, Mississippi; prepared under contract for Defense Nuclear Agency by University of Illinois, Urbana, Illinois; Unclassified.

8. A. J. Hendron, Jr., and others; "Geomechanical Model Study of the Behavior of Underground Openings in Rock Subjected to Static Loads; Tests on Lined Openings in Jointed and Intact Rock"; Contract Report N-69-1, Report 3, June 1972; U. S. Army Engineer Waterways Experiment Station, CE, Vicksburg, Mississippi; prepared under contract for Defense Nuclear Agency by University of Illinois, Urbana, Illinois; Unclassified.

9. D. U. Deere and R. P. Miller; "Engineering Classification and Index Properties for Intact Rock"; Technical Report No. AFWL-TR-65-116, December 1966; Air Force Weapons Laboratory, Kirtland Air Force Base, New Mexico; Unclassified.

10. J. Handin and R. V. Hager, Jr.; "Experimental Deformation of Sedimentary Rocks Under Confining Pressures: Tests at Room Temperature on Dry Samples"; Bulletin of American Association of Petroleum Geologists, January 1957, Vol. 41, No. 1, Pages 1-50; Unclassified.

11. J. Handin and others; "Experimental Deformation of Sedimentary Rocks Under Confining Pressure: Pore Pressure Tests"; Bulletin of American Association of Petroleum Geologists, May 1963, Vol. 47, No. 5, Pages 717-755; Unclassified.

12. E. C. Robertson; "Experimental Study of the Strength of Rocks"; Bulletin of the Geological Society of America, October 1955, Vol. 66, Pages 1275-1314; Unclassified.

13. A. F. Dorris; "Response of Horizontally Oriented Buried Cylinders to Static and Dynamic Loading"; Technical Report No. 1-682, July 1965; U. S. Army Engineer Waterways Experiment Station, CE, Vicksburg, Mississippi; Unclassified.

In accordance with ER 70-2-3, paragraph 6c(1)(b), dated 15 February 1973, a facsimile catalog card in Library of Congress format is reproduced below:

Wallace, James G
Behavior of lined openings in jointed and unjointed model rock masses, by J. G. Wallace. Vicksburg, Miss., U. S. Army Engineer Waterways Experiment Station, 1973.
56 p. illus. 27 cm. (U. S. Waterways Experiment Station. Technical report N-73-6)
Sponsored by Office, Chief of Engineers, U. S. Army, Project No. A880.
References: p. 55-56.
1. Joints and joining (Geology). 2. Lined tunnels. 3. Models. 4. Rock masses. 5. Static pressure. I. U. S. Army. Corps of Engineers. (Series: U. S. Waterways Experiment Station, Vicksburg, Miss. Technical report N-73-6)
TA7.W34 no.N-73-6